UiT
THE ARCTIC
UNIVERSITY
OF NORWAY

Molecular Pharmacology and Toxicology

Faculty of Health Sciences

Allosteric modulation of GABAergic and glutamatergic metabotropic receptors

—

Thibaud Freyd

A dissertation for the degree of Philosophiae Doctor – June 2018

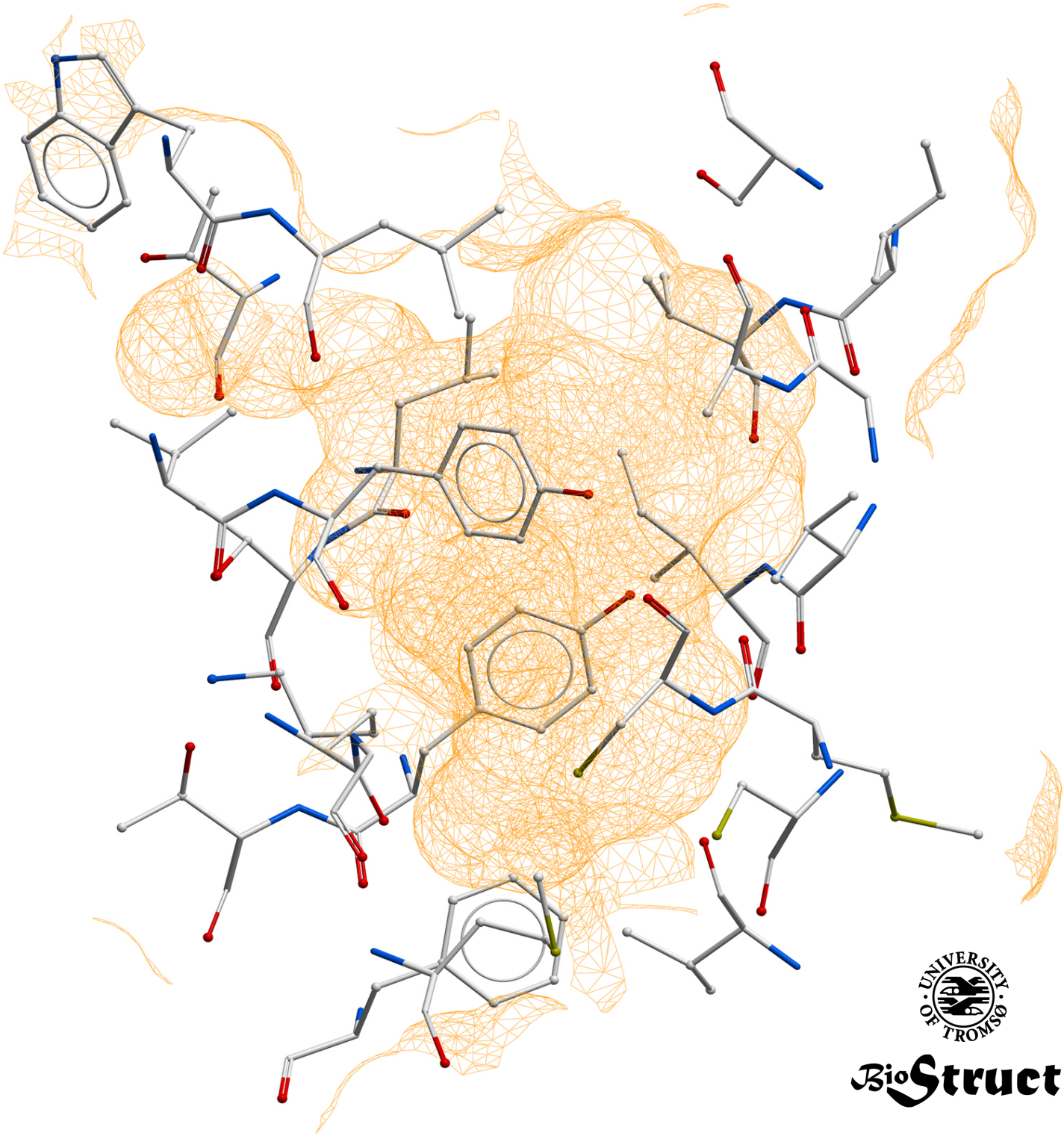

UNIVERSITY OF TROMSØ

BioStruct

Content

Acknowledgments

It is finally my turn to write this section of the actual thesis. A Ph.D. is said to be a personal work, but in my opinion, it is the result of a long teamwork with all the people I worked with along the course, and also the ones I met on a personal level.

I express my deepest gratitude to my supervisors who helped me achieve this Ph.D. Professor Ingebrigt Sylte, thank you for guiding me and for always keeping your door open, for answering my questions and wonders. Your good nature and optimism are gifts that helped me through the Ph.D. I thank Dr. Mari Gabrielsen, for her guidance and perseverance. Your attention to detail rescued me more than once. I enjoyed learning under the supervision of both of Mari and Ingebrigt. You never gave up on me despite my franglish (:D)!

I would also like to thank Associate Professor Kurt Kristiansen for his support with Linux and Dr. Imin Wushur for the incredible work he has done with the *in vitro* experiments.

The work presented in this thesis would not have been possible without our collaborators in Poland and France. I would like to thank the research group of Professor Andrzej J. Bojarski, with special thanks to Dr. Dawid Warszycki and Dr. Stephan Mordalski. The help of Johann Hendrickx (UMR CNRS 6286, France) was highly beneficial for the results obtained in paper 3.

I would like to thank all my office mates. Krishanthi, next time I see you I will bring “pain” and “poisson”. Linn, please do not involve me in more Snapchat videos!

I also want to thank all my friends in Tromsø for making my stay in this town memorable.

To my family, merci de votre soutien constant et de votre patience. Papa, Maman, si vous lisez ce texte, ça veut dire que j’ai enfin la réponse à votre question “Tu finis quand ?”.

Last but not least, to my fiancée Maria Rini. Thank you for your patience and commitment despite the distance between us. You braved Norway's cold weather for me and I know it was hard for you. Notre future change le 20.10.18!

This study was supported by the Polish-Norwegian Research Programme operated by the Polish National Centre for Research and Development under the Norwegian Financial Mechanism 2009–2015 in the frame of Project PLATFORMex (Pol-Nor/198887/73/2013), and by Helse Nord project number HNF1426-18. The project was also supported by HPC resources from NOTUR- project NN2978K, and by the PhD school Biostruct and UiT The Artic University of Norway in Tromsø.

Tromsø, June 2018
Thibaud Freyd.

List of papers

The PhD thesis is based on the following papers:

I. **Freyd, T.**, Warszycki, D., Mordalski, S., Bojarski, A.J., Sylte, I and Gabrielsen, M (2017)

Ligand-guided homology modelling of the $GABA_{B2}$ subunit of the $GABA_B$ receptor.

PLoS One, DOI 10.1371/journal.pone.0173889

II. **Freyd, T.**, Wushur, I., Evenseth, L.M., Warszycki, D., Brandski P., Pilc, A., Bojarski, A.J., Gabrielsen, M. and Sylte, I. (2018)

A virtual ligand screening approach for new $GABA_B$ receptor modulators.

Manuscript.

III. Freyd, T., Hendrickx, J., Sylte, I and Gabrielsen, M. (2018)

Opening of an intracellular water channel in the metabotropic glutamate receptor 1 by a positive allosteric modulator with intrinsic agonist properties.

Manuscript.

Abbreviations

β_2-AR: beta-2 adrenergic receptor

7TM: seven transmembrane domain

ADMET: Administration Distribution Metabolism Excretion Toxicity

agoPAM: agonist positive allosteric modulator

AMPA: α-amino-3-hydroxy-5-methyl-isoxazole-4-propionate

AMs: allosteric modulators

BBB: Blood-brain barrier

BEDROC: Boltzmann-enhanced discrimination of receiver operating characteristic

CADD: computer-aided drug design.

cAMP: cyclic adenosine monophosphate

CHO: Chinese hamster ovary

CNS: Central Nervous System

CPU: central processing unit

EAATs: excitatory amino acid transporters

ECL: extracellular loop

ERS: endoplasmic retention sequence

G-protein: guanine nucleotide binding protein

GAT: GABA transporter

GABA: γ-aminobutyric acid

$GABA_B$-R: $GABA_B$ receptor

GDP: guanosine diphosphate

GIRK: inwardly-rectifying potassium

GPCR: G-protein coupled receptor

GPCRdb: G-protein coupled receptor database

GPGPU: general-purpose graphic processing unit

GRK: G-protein-coupled receptor kinase

GTP: guanosine triphosphate

HTS: high-throughput screening

ICL: intracellular loops

IUPHAR: International Union of Basic and Clinical Pharmacology

K^+: potassium ion

KA: kainate

MD: molecular dynamics

mGlu-R: metabotropic glutamate receptor

MM: molecular mechanics

MDD: major depressive disorder

MM-GBSA: molecular mechanics-generalized Born surface area

MSA: multiple sequence alignment

NAM: negative allosteric modulator

NMDA: N-methyl-D-aspartate

PAM: positive allosteric modulator

PDB: protein data bank

QM: quantum mechanics

RO5: rule of five

SAR: structure–activity relationship

SBDD: structure-based drug-design

SID: simulation interaction diagram

SIFt: structural interaction fingerprints

Tc: Tanimoto coefficient

vdW: van der Walls

VFT: Venus Flytrap

VGCCs: voltage gated calcium channels

VMD: Visual Molecular Dynamics

VS: virtual screening

Vsw: Virtual Screening Workflow

Summary

G-protein coupled receptors (GPCRs) are targets for 1/3 of the drugs available on the market making research on this class of proteins a very hot topic in the field of drug discovery. γ-amino butyric acid (GABA) and glutamate are respectively the main inhibitory and the main excitatory neurotransmitters in the mammalian central nervous system (CNS). The $GABA_B$ receptor ($GABA_B$-R) and the metabotropic glutamate receptors 1-8 ($mGlu_{1-8}$-Rs) belong to family C GPCRs and are functional dimers. They are potential drugs targets for the treatments of CNS disorders among others. $GABA_B$-R is also involved in drug and alcohol addictions. The actual therapeutic treatments for CNS diseases come with serious side-effects due to off-target binding. Allosteric modulators (AMs) might hold the opportunity to design more selective drugs with less unwanted effects as the allosteric binding sites are less conserved than orthosteric binding sites. An allosteric binding site has been identified in $GABA_B$-R and mGlu-Rs. The 3D structure of the $GABA_B$-R is unknown while experimental structures of the $mGlu_1$-R and $mGlu_5$-R are available. Though, the activation mechanism of these receptors remains unclear to this date.

In the first part of the present study, using the computational technique of homology modelling, several spatial conformations of the subunit $GABA_{B2}$ were predicted. These theoretical 3D models were used to map the residues of the putative allosteric pocket of $GABA_B$-R. They were also employed in a ligand- and structure-based virtual ligand screening to retrieve potential AMs for the $GABA_B$-R within a database of 8 million commercial compounds. 55 compounds were bought and the experimental testing confirmed that 8 of the identified compounds act as allosteric modulators for the $GABA_B$-R.

In the last part of this study, the experimental structure of $mGlu_1$-R was employed as a model to investigate the activity mechanism of several AMs. Using the computational technique of non-biased molecular dynamics (MD) simulation, several partially overlapping binding pockets were identified. The role of water molecules was also demonstrated to be critical for the protein-ligand interactions and activation. One of the AMs with agonist activity induced the opening of a water channel extended from the cytosol up to a region proposed to be important for activation. These results are in lines with other studies performed on GPCR family A members.

The presentation of the first AMs discovered via *in silico* efforts and the allosteric pocket for the $GABA_B$-R will be of big help for future drug discovery campaigns. The

results of the MD simulations might help to find a general mechanism of activation for the GPCRs.

1. Introduction

The adult human central nervous system (CNS) contains approximately 86 billion nerve cells (neurons) (Herculano-Houzel, 2009), that communicate with each other via chemical synapses. The communication requires release of chemical substances, neurotransmitters, which interact with membrane proteins called neurotransmitter receptors. These receptors are located both in pre- or post-synaptic cellular membranes. Some neurotransmitters trigger the firing of the neurons by depolarisation of the cellular membrane while other trigger inactivation of the neuron by hyperpolarisation of the cellular membrane. So far, more than 100 different neurotransmitters have been identified and categorized into two broad categories: neuropeptides and small-molecule neurotransmitters (Purves et al., 2001). In the last category, we find the biogenic amines (dopamine, noradrenaline, epinephrine, histamine and serotonin) and the amino acids, which includes neurotransmitters such as γ-amino butyric acid (GABA) and glutamate (Purves et al., 2001). Two mains groups of neurotransmitter membrane receptors coexist: 1.- ionotropic receptors (ligand-gated ion channels) giving fast responses lasting for a few milliseconds (e.g. reflexes). 2. - metabotropic receptors (G-protein coupled receptors) giving slower and longer lasting responses than the ionotropic receptors.

1.1. Glutamate and GABA neurotransmitters in the CNS

Glutamate is the main excitatory neurotransmitter in the mammalian CNS (Pol et al., 1990). Glutamate is synthesised locally in the axon terminal, due to its incapacity to cross the brain blood barrier (BBB), and is released into the synaptic cleft upon depolarisation. The glutamate reuptake is performed by transporter proteins, located in the membrane of glial cells and in presynaptic neurons, called excitatory amino acid transporters (EAATs).

Glutamate exerts its function by activating ionotropic receptors that mediate fast excitatory synaptic transmission. Autoregulatory receptors on the presynaptic neuron regulate the increase or decrease of neurotransmitter release. So far, three ionotropic glutamate receptors have been identified and named after their pharmacological profile: ionotropic N-methyl-D-aspartate (NMDA), α-amino-3-hydroxy-5-methyl-isoxazole-4-propionate (AMPA) and kainate (KA) receptors (D T Monaghan et al., 1989; Hollmann and Heinemann, 1994).

The glutamate receptor family also contain eight metabotropic receptors ($mGlu_{1-8}$-Rs) responsible for slow synaptic activation (seconds) and cellular excitability. The mGlu-Rs are subdivided into three subgroups according to their sequence homology, pharmacological profile and guanine nucleotide binding protein (G-protein) coupling. Group I, consisting of $mGlu_1$- and $mGlu_5$-R, are located predominantly postsynaptic (Pittaluga, 2016) and are responsible for excitation. When activated, $mGlu_1$- and $mGlu_5$-R couple with G_q and G_{11} G-proteins giving stimulation of the phospholipase C (PLC) signalling cascade and triggering of calcium mobilization from endoplasmic reticulum that leads to firing of postsynaptic neurons (Niswender and Conn, 2010). Group II, consisting of $mGlu_2$- and $mGlu_3$-R and group III, consisting of $mGlu_{4-6-7-8}$-Rs, are usually located on presynaptic neurons as auto- or hetero receptors. Group II as well as $mGlu_4$- and $mGlu_8$- have also been described to be expressed on postsynaptic neurons (Bradley et al., 1996; Koulen and Brandstätter, 2002; Muly et al., 2007), where they couple with the G_i and G_o G-proteins and inhibit adenylate cyclase, resulting in decreased release of neurotransmitters into the synaptic cleft and reduction of the excitability of postsynaptic neurons (Niswender and Conn, 2010). For all mGlu-Rs, exceptions of the expression, localisation and G-protein coupling described above can be seen in several areas of the brain (see examples in Niswender and Conn, 2010), and only general trends are listed above. For instance, $mGlu_5$-R was demonstrated to be capable of forming weak G_s coupling when activated by the agoPAM VU0424465 (Nasrallah et al., 2018). An agoPAM is a positive allosteric modulator (PAM) with agonist activity (see below).

GABA is synthetized from glutamate and in general is giving the opposite effect of glutamate, as GABA is the main inhibitory neurotransmitter in the mammalian CNS. GABA exerts its biological functions by activation of three types of membrane receptors: the ionotropic receptors $GABA_A$ and $GABA_C$ and the metabotropic $GABA_B$ receptor ($GABA_B$-R). The action of GABA in the synaptic cleft is terminated by reuptake by the GABA transporters (GAT) located in the neurons and glial cells (see review Krirschuk and Kilb, 2012; Scimemi, 2014). The $GABA_B$-R is expressed on both pre- and post-synaptic neurons and couples to the G_i and G_o G-proteins. When activated, $GABA_B$-R inhibits adenylate cyclase giving a decrease in intracellular cAMP levels (Figure 1).

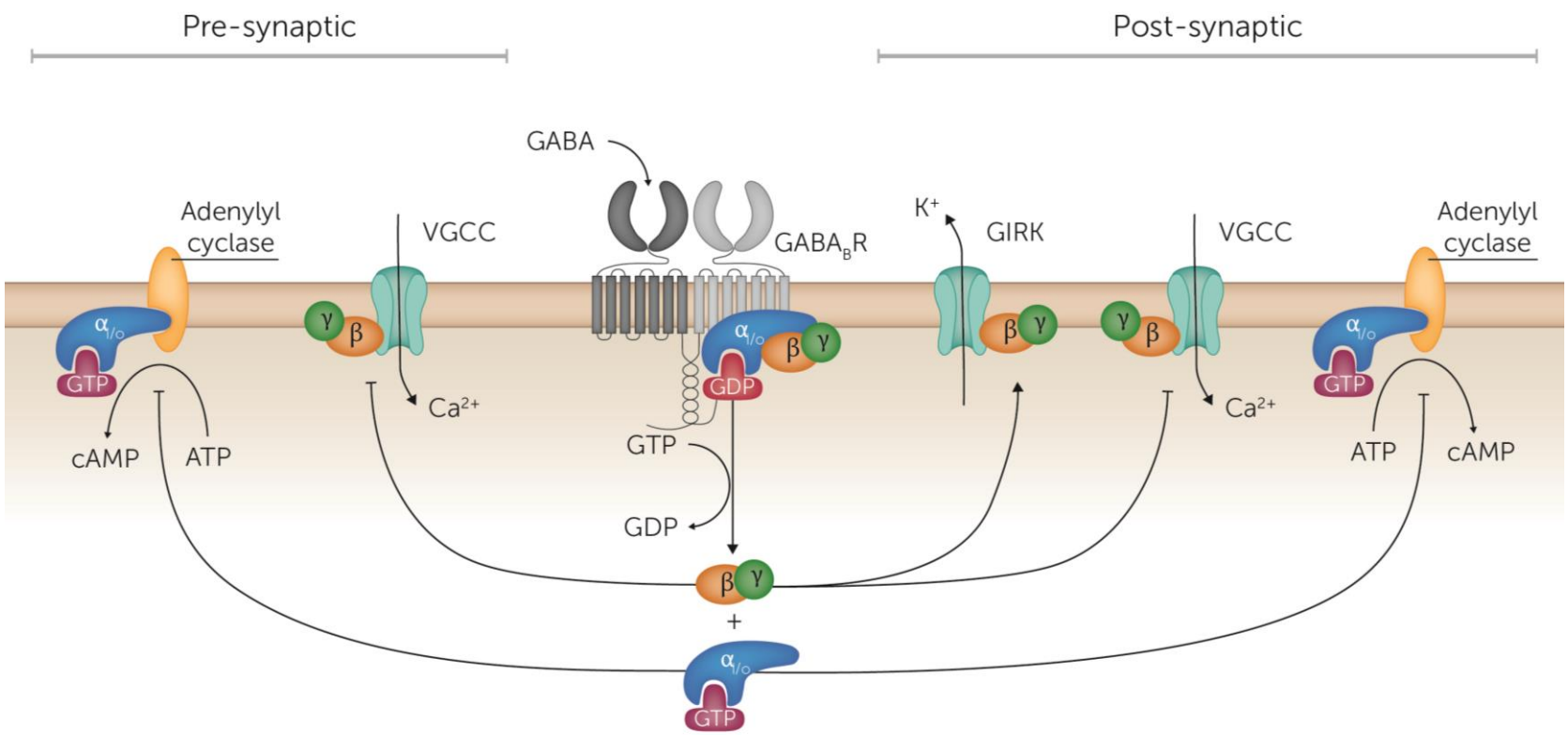

Figure 1: Effectors of the GABA$_B$ receptors. *Effects of the GABA$_B$ receptor activation when located in presynaptic/postsynaptic neuron. ATP: Adenosine Triphosphate, cAMP: Cyclic adenosine monophosphate, GDP: Guanosine Diphosphate, GTP: Guanosine Triphosphate, VGCC: Voltage Gated Calcium Channels, GIRK: G-protein-coupled inwardly-rectifying potassium. (modified from Gassmann and Bettler, 2012).*

The presynaptic $GABA_B$-Rs function as auto- and hetero receptors, and the activation results in reduced neurotransmitter release, primarily through the inhibition of calcium-dependent neurotransmitter release. Presynaptic activation not only reduces the release of GABA, but also the release of serotonin, noradrenaline and dopamine (Conn et al., 2014). The G_α subunit inhibits adenylyl cyclase while the $G_{\beta\gamma}$ complex inhibits voltage gated calcium channels (VGCCs) (Figure 1) (Kohl and Paulsen, 2010).

Activation of postsynaptic $GABA_B$-R results in inhibition of adenylate cyclase and triggers the opening of G-protein-coupled inwardly-rectifying potassium (GIRK) channels via $G_{\beta\gamma}$ activity, leading to K^+ efflux and hence hyperpolarisation (Figure 1).

The eight mGlu-Rs and the $GABA_B$-R s all belong to family C of G-protein coupled receptors (GPCRs), and share the same structural and mechanistic characteristics.

1.2. G-protein coupled receptors

The GPCR superfamily is one of the largest and oldest, and members are found in all kingdoms: animal, plant, fungi and protozoa (Perez, 2003; Xue et al., 2008). Studies have estimated that 2 % percent of the human genome is coding for GPCRs, giving more than 800 human GPCRs (Fredriksson et al., 2003). GPCRs are transmembrane proteins sharing a motif of seven transmembrane α-helixes. Their role is to transduce external stimulus to the inside of the cell. GPCRs are activated by a variety of ligands: from photons and ions to neurotransmitters, lipids and peptides. GPCRs obtained their name since it was discovered that upon activation they couple to G-proteins at the intracellular side of the membrane. GPCRs have also been seen to undergo conformational change and G-protein coupling without external stimulus present (see review Costa and Cotecchia, 2005), which is known as constitutive activity. GPCRs can also activate other signalling pathways by coupling to arrestins (see below). GPCRs are involved in the regulation of a wide variety of cellular and physiological functions, which means they are also involved in numerous pathological processes which explains why this protein class is the most studied for drug discovery (see overview Hauser et al., 2017). About 1/3 of the drugs on the market target GPCRs (Hauser et al., 2017; Overington et al., 2006) but the targeted GPCRs represent only a fraction of the GPCRs expressed in the human body (Hauser et al., 2017).

1.2.1. G-protein coupled receptor families

The International Union of Basic and Clinical Pharmacology (IUPHAR) is responsible for an international classification system for human GPCRs. The classification is based on

the amino acid sequences similarities of their transmembrane domain; hence they are divided into 5 mains families (or classes). The classification system is often termed the GRAFS classification based on the names of the families as follows: Glutamate (family C), Rhodopsin (family A), Adhesion, Frizzled (family F) and Secretin (family B) (Civelli et al., 2013; Gloriam et al., 2007). Another overlapping classification system is also used that splits GPCRs into a clan system from A to F. The largest family is family A containing all receptors binding biogenic amine neurotransmitters, peptides and hormones as well as the receptors responsible for vision, olfaction and type 2 taste receptors. Family B mainly consists of receptors activated by peptides. Family C contains receptor activated by amino neuromodulators, calcium and pheromones and the taste receptors of type 1. The members of each family are then subdivided according to sequence similarities, pharmacological profiles and G-protein coupling. Numerous orphan receptors with unknown endogenous ligands are also found within the families A and C (Pándy-Szekeres et al., 2018).

1.2.2. Activation of signalling pathways

GPCRs are known to adopt multiple conformations depending on the ligand bound, and one receptor may couple to several signalling cascades. According to the conformation adopted upon activation, the triggered intracellular signalling cascade differs, and is now distinguished between G-protein-dependant signalling and G-protein independent signalling (Figure 2, Hilger et al., 2018).

G-proteins are heterotrimeric proteins consisting of the subunits G_α, G_β and G_γ. In the inactive form, all subunits are found as a heterotrimer located at the membrane with a guanosine diphosphate (GDP) bound at the G_α subunit. The activation of GPCR triggers a conformational change of the 7TM bundle and then the coupling with a G-protein. The GPD is exchanged for a guanosine triphosphate (GTP) followed by the dissociation of the heterotrimer to G_α-GTP and the dimer $G_{\beta\gamma}$. Each subunit interacts with its target(s), the effectors. Effectors are enzymes or ion channels that modulate the levels of molecules often called the second messengers. The G_α subunit has a GTPase activity and as such, cleaves GTP to GDP which triggers the deactivation of the G protein and the reassembly of the subunits as a heterotrimeric complex (Figure 2, Oldham and Hamm, 2008).

Activation of a GPCR may also leads to coupling to arrestins and thus, to activation of G-protein independent pathways. The GPCR needs to be phosphorylated by a G-protein-coupled receptor kinase (GRK) at the intracellular part of the receptor before coupling

with an arrestin. There are four subtypes of arrestins (arrestin 1-4). Arrestin-2 and arrestin-3 are also called β-arrestin1 and β-arrestin2. Arrestins are activated by coupling with a phosphorylated GPCR. Once formed, the GPCR-arrestin complex triggers arrestin-dependant signalling pathways such as activation of mitogen-activated protein kinases (MAPKs) or SRC kinases (Hilger et al., 2018). The coupling to arrestin can also lead to internalisation of the complex for GPCR recycling or degradation (Figure 2). For full review of both type of signalling pathways please see Hilger et al., 2018.

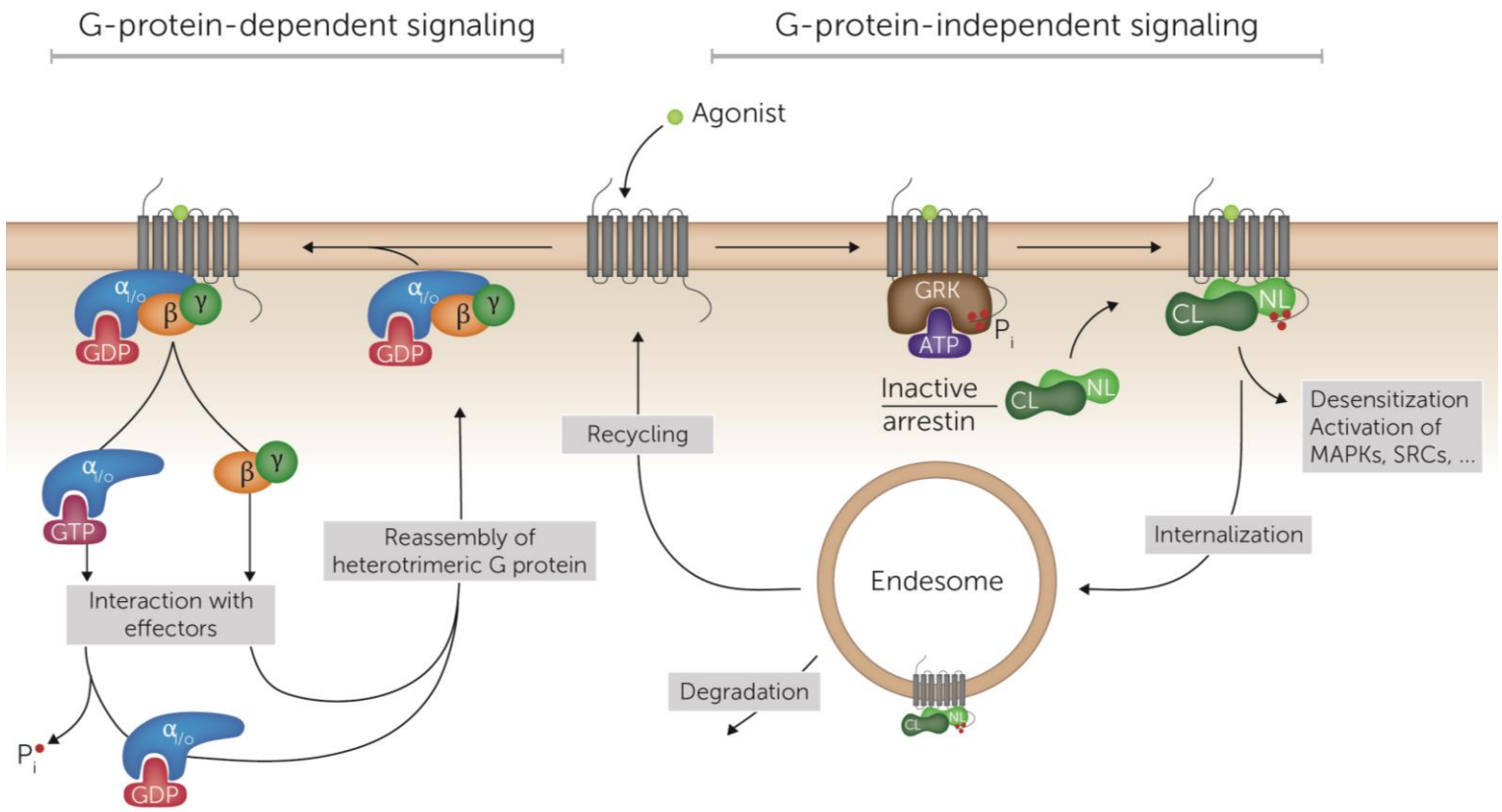

Figure 2 G-protein-coupled receptor signal transduction. *Illustration of the G-protein-dependant and -independent signalling pathways upon GPCR activation. ATP: Adenosine Triphosphate, GTP: Guanosine Triphosphate, GDP: Guanosine Diphosphate, GRK: G-protein-coupled receptor kinase, NL: N lobe of arrestin, CL: C lobe of arrestin, MAPKs: mitogen-activated protein kinases. (modified from Hilger et al., 2018.)*

1.2.3. General structural knowledge

The GPCRs are also named 7TM receptors since they share a common domain of 7 membrane-spanning segments conserved through the evolution despite quite low amino acid sequence similarities (<15% between family A and C, Paper 1). The membrane spanning segments constitutes of 7 transmembrane α helices (TM), labelled TM 1-7 from the N- to the C-terminus (Figure 3). The helices are linked to each other by intracellular and extracellular loops (ICL 1-3 and ECL 1-3 respectively, Figure 3). Some of the GPCRs have an eighth helix located at the C-terminal intracellular part and parallel to the lipid membrane. The pattern of TM organization is the same in all GPCR families, generating a circular bundle with the N- and C-termini located extracellularly and intracellularly, respectively.

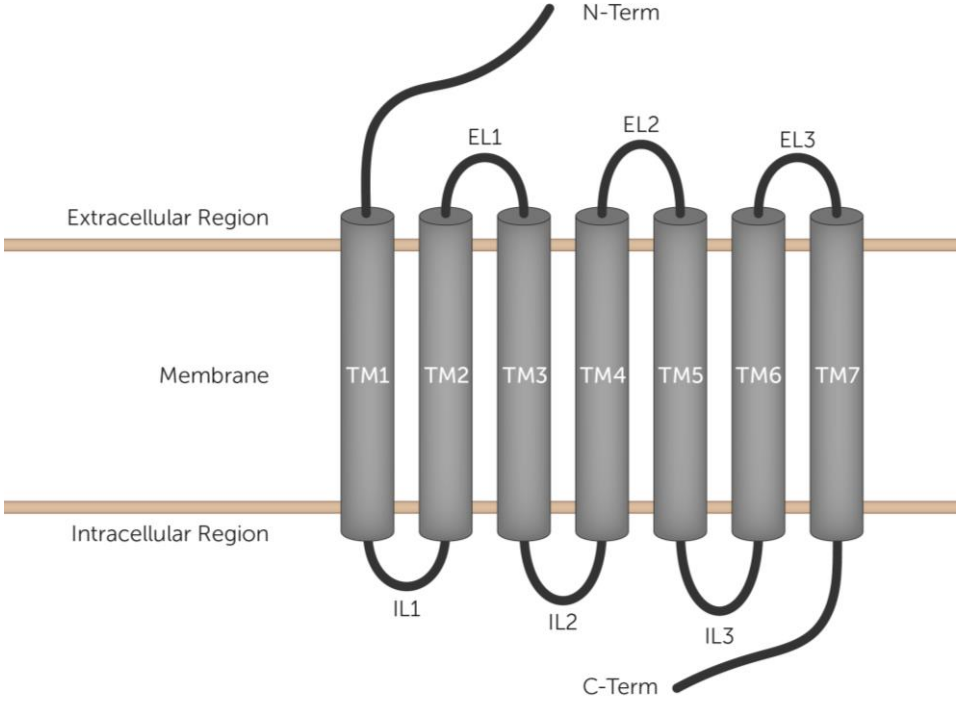

Figure 3 Schematic view of the organisation of the termini, loops and 7 TM helices of a GPCR.TM: Transmembrane helix, EL: Extracellular Loop, IL: Intracellular Loop (modified from Gacasan et al., 2017)

Up to the year of 2000, the structural knowledge about GPCRs was limited and was based on indirect knowledge from molecular biology studies, amino acid sequence analysis and the electron microscopy maps of rhodopsin (see review Costanzi et al., 2009). The release of the x-ray crystal structure of the membrane domain of bovine rhodopsin in 2000 was a major breakthrough (Palczewski et al., 2000). Other important breakthroughs in the field was the release of the x-ray crystal structure of an engineered

human β_2-adrenergic receptor (β_2-AR, Cherezov et al., 2007) in complex with the agonist carazolol, and later the human β_2-AR coupled with a bovine G_s G-protein (Chung et al., 2011) as well as the experimental structure of rhodopsin bound to arrestin (Kang et al., 2015). In addition, the first representatives of the family B (Siu et al., 2013), C (Doré et al., 2014; Wu et al., 2014) and Fizzled members (Wang et al., 2013) were resolved in 2013, 2014 and 2013 respectively.

At present (June, 2018), 252 GPCR x-ray crystal structures of 67 unique receptors are available in the PDB with a majority belonging to family A (Pándy-Szekeres et al., 2018). Only 20% of the 252 x-ray structures are in an active conformation (from family A and B), the others being either in an intermediate state or an inactive conformation. Recently, four experimental structures of GPCRs bound to their G-protein were resolved by cryo electron microscopy (cryo-EM): the human rhodopsin, human adenosine A_1 and μ-opioid receptors bond to the G-protein G_i (Draper-Joyce et al., 2018; Kang et al., 2018; Koehl et al., 2018) as well as the serotonin 5-HT_{1B} receptor coupled to the G_o G-protein (García-Nafría et al., 2018).

In spite of the low sequence similarities between the TM helices of the GPCRs, the helical packing is very well conserved throughout the entire superfamily (Cvicek et al., 2016), and multiple sequences motifs are also conserved within each of the families. Based on family A studies, an active conformation of a GPCR is primarily characterised by an outward movement of the intracellular part of TM6 compared to the inactive conformation, which opens the binding pocket for the G-protein (Rasmussen et al., 2011). Based on the analysis of active and inactive x-ray crystal structures of rhodopsin, muscarinic M2 and β_2-AR receptors, Cvicek *et al.* identified that the difference between an active and an inactive conformation could be resumed to changes in terms of molecular contacts involving only 15 different residues (Cvicek et al., 2016).

1.3. Family C of G-protein coupled receptors

1.3.1. General structure and binding pockets

GPCRs members of the family C are functional dimers. Compared to family A, family C receptors possess an additional domain located at the N-terminus, termed the Venus Flytrap (VFT). The binding pocket for endogenous ligands, also named the orthosteric binding pocket, is located within the 7TMs of family A receptors. For family C, this binding pocket is located in the VFT (Figure 4). The VFT is connected to the 7TM domain via a

cysteine-rich linker domain (CRD), however, this domain is lacking in the $GABA_B$-R (Figure 4). An allosteric binding pocket has been described and confirmed experimentally within the 7TM bundle, located in a region corresponding to the orthosteric binding pocket of family A (Doré et al., 2014; Wu et al., 2014).

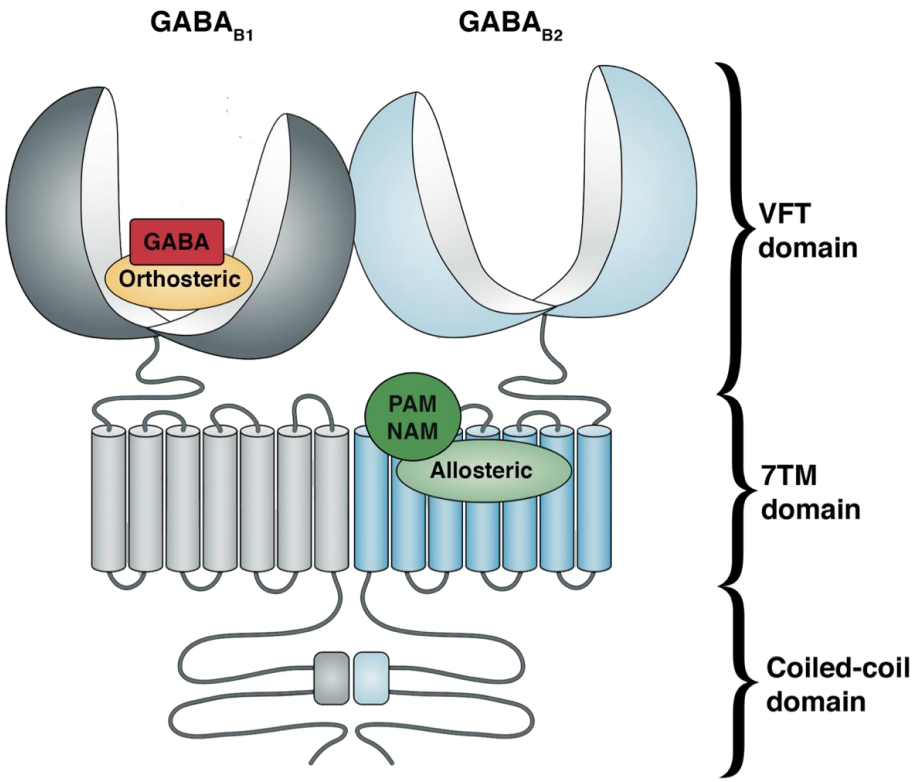

Figure 4 illustration of a GPCR family C member, the $GABA_B$-R (modified from Conn et al., 2009)

1.3.2. The $GABA_B$ receptor

1.3.2.1. Structural knowledge

$GABA_B$-R is a functional heterodimer of two protomers ($GABA_{B1a}$ or $GABA_{B1b}$ and $GABA_{B2}$, (Robbins et al., 2001). Two ligand-binding sites have been characterised for the $GABA_B$-R. GABA and other orthosteric compounds bind to the extracellular VFT of $GABA_{B1}$ (Brown et al., 2015). The allosteric modulators (AMs) bind $GABA_B$-R in a binding site mapped in the 7TM domain of the $GABA_{B2}$ (Figure 4) (Binet et al., 2004; Dupuis et al., 2006). The dimer of the VFT domains of $GABA_B$-R as well as the VFT of the $GABA_{B2}$ alone (Geng et al., 2012) were resolved by x-ray crystallography in apo form and in complex with agonists or antagonists (Geng et al., 2013). These crystal structures showed that the VFT of the $GABA_{B1}$ closes upon binding of an agonist, while antagonists stabilise an open $GABA_{B1}$ VFT conformation. The VFT of $GABA_{B2}$ remains in an open state both when

agonists or antagonists bind the VTF of $GABA_{B1}$. No orthosteric binding site is present in the VFT of $GABA_{B2}$ (Kniazeff et al., 2002), which is responsible for coupling to G proteins (Galvez et al., 2001). To date, no experimental structures of the heptahelical domain of the $GABA_B$-R is available.

$GABA_{B1}$ cannot be expressed alone at the membrane due to the presence of an endoplasmic retention sequence (ERS) at its C-terminal (Margeta-Mitrovic et al., 2000). The ERS is hidden through a coil-coil interaction when both subunits are presents (Calver et al., 2001; Pagano et al., 2001).

1.3.2.2. $GABA_B$ receptor as drug target

The $GABA_B$-R is considered as a putative target for new drug development in numerous neurological and neuropsychiatric disorders including anxiety and depression, epilepsy, autism spectrum disorders, drug and alcohol addiction, schizophrenia, as well as other conditions such as muscle spasticity, gastrointestinal reflux disorder, and pain (Brown et al., 2015; Cryan and Kaupmann, 2005; Lehmann et al., 2012). The $GABA_B$-R has been linked with depression for 30 years (see review Ghose et al., 2011). The $GABA_B$-R as a pharmacological target in anxiety and major depressive disorder (MDD) has been controversial since both agonists and antagonists have shown to exhibit antidepressant activity (Frankowska et al., 2007). The $GABA_B$-R has a very complex signalling network and different signalling systems are dominating in different brain regions (Gassmann and Bettler, 2012; Pin and Bettler, 2016). As a consequence, an active compound may create diverse and sometimes opposite effects depending on where the compound acts, and the dominating signalling system in that area. This may also explain that both agonists and antagonists have shown antidepressant effects.

The only marketed drug targeting the $GABA_B$-R is the orthosteric compound baclofen, a selective agonist (Bowery, 1993). Baclofen is used to treat spasticity (Penn and Kroin, 1987) and has also been demonstrated to treat alcohol dependence (Morley et al., 2014; Pastor et al., 2012). No antagonists or AMs targeting the $GABA_B$-R have yet been marketed as a drug but several are at the stage of clinical trials (see below).

1.3.3. Metabotropic glutamate receptors

1.3.3.1. Structural knowledge

Like the $GABA_B$-R, the mGlu-Rs are functional dimers. For a long time, it was anticipated that mGlu-Rs only form homodimers, however, recently it was discovered

that they also can form heterodimers (Doumazane et al., 2010; Moustaine et al., 2012; Yin et al., 2014). A study showed that the pharmacological profile of the heterodimer is different from the homodimers. For instance, the $mGlu_2$:$mGlu_4$-R heterodimer showed a pharmacological profile different from that of the $mGlu_2$-R and $mGlu_4$-R homodimers (Yin et al., 2014). Within a dimer (both homo- and heterodimers), only one of the protomers couples with G-proteins upon activation (Moustaine et al., 2012).

The VFT domains of most mGlu-Rs have been solved by x-ray crystallography, while the 7TM domains of $mGlu_1$-R (Wu et al., 2014) and $mGlu_5$-R (Christopher et al., 2015, 2018; Doré et al., 2014) are known from x-ray crystallography. In the x-ray structure of the TM domain of the $mGlu_1$-R (Wu et al., 2014), the receptor is found as a homodimer, however, the interface of contacts between the two protomers may be an artefact of the crystallisation process as described by a paper investigating the promoters interface by cysteine cross-linking of the $mGlu_2$-R (Xue et al., 2015).

1.3.3.2. Metabotropic glutamate-receptors as drug target

The wide distribution of metabotropic glutamate receptors throughout the CNS is linking the mGlu-Rs to numerous brain functions and hence to dysfunctions. Dysfunction of glutamatergic neurotransmission is connected to numerous CNS disorders (for review see Gregory et al., 2013; Niswender and Conn, 2010) such as depression (Pilc et al., 2008), anxiety (Swanson et al., 2005), schizophrenia (Moghaddam, 2004), Parkinson disease (Masilamoni and Smith, 2018), L-DOPA-induced dyskinesia (Sebastianutto and Cenci, 2018), Fragile X syndrome (Michalon et al., 2012), and epilepsy (Alexander and Godwin, 2006; Ngomba and van Luijtelaar, 2018).

The distribution of mGlu-R subtypes is not homogenous in the brain, so targeting the correct subtype is necessary for a successful treatment of a disease. For instance, group I mGlu-Rs are connected to depression, while group II is connected to anxiety and schizophrenia. Group III members have been linked to Parkinson disease, addiction and depression (Gregory et al., 2013; Niswender and Conn, 2010).

1.4. Mechanism of GPCR activation

GPCRs show constitutive activity, indicating that they are in equilibrium between populations of inactive and active receptor conformations without external stimuli present (Costa and Cotecchia, 2005). Different chemical compounds induce different receptor conformations, changing the equilibrium between active, intermediate and

inactive conformations. Most of the mechanistic activation features are protein specific, or family specific, but some features are accepted as common among GPCRs.

1.4.1. Family A

The first available 3D structures of GPCRs in active conformations were family A members, and most of the publications concerning mechanism of activation were from this family. A list of all active GPCRs 3D structure is available on the website of the GPCRdb (Pándy-Szekeres et al., 2018). At present, (June, 2018) 17 active state receptor 3D structures are available, but only for family A and B.

The most obvious difference between active and inactive conformations is a large outward movement of the intracellular part of TM6 in the active conformation compared with the inactive. This movement allows G-protein to interact with the receptor. An ionic lock is present in approximately 50 % of all family A GPCRs, and the outward movement of TM6 requires a breakage of the ionic lock. The ionic lock is formed between two well-conserved charged amino acids: an arginine from the D/ERY motif in position 3.50a (TM3), and a D/E in position 6.50a (TM6) (Trzaskowski et al., 2012).

Upon activation, $W^{6.48a}$, from the CWxP motif found in TM6, is moved inward (Trzaskowski et al., 2012), but this movement is not seen in all x-ray crystal structures of activate GPCRs and was not proposed as a common activation feature.

The motif NPxxY at the intracellular end of TM7 is known as the activation switch. During activation of family A members, $Y^{7.53a.48c}$ (Y in NPxxY) is moved inward to fill up the space created by the outward movement of TM6 (Rasmussen et al., 2011; Trzaskowski et al., 2012). This switch is also named the “tyrosine toggle switch” in the scientific literature.

A hydrophobic hindering mechanism (HHM) involving the position F6.44a, L3.43a and X6.40a (with X a bulky amino acid) was also proposed. It was suggested that during activation there is rearrangements of these residues and creation of a water channel within the receptor (Tehan et al., 2014). Another study also found that the reorganisations of hydrophobic amino acids receptor during the activation process permits the creation of a water channel. One of these rearrangements was identified to $Y^{7.53a}$ from the NPxxY motif (Yuan et al., 2014).

1.4.2. Family C

1.4.2.1. VFT

The first step in the activation of family C GPCRs is closing and stabilisation of the VFT. For $GABA_B$-R, only $GABA_{B1}$ binds GABA, while both protomers of an mGlu-R dimer bind glutamate. The closing of $GABA_{B1}$-VFT is enough for full activation of the $GABA_B$-R. For mGlu-R, the closing of one VFT is enough for getting an activate receptor but is not sufficient for maximal activation of the receptor (Kniazeff et al., 2004).

After closing of $GABA_{B1}$-R, the VFT is reoriented and inter-contacts between the two lower lobes of $GABA_{B1}$-R and $GABA_{B2}$-R are formed. The CRD linking the VFT domains and the 7TM domain was demonstrated to be necessary for an the allosteric communication between the VFT domain and the 7TM domains of the mGlu-Rs (Rondard et al., 2006). The molecular mechanism of signalling between the VFTs and the 7TM domains is still unknown both for $GABA_B$-R and the mGlu-Rs (Rondard et al., 2017). Studies on mGlu receptors and other family C members have shown that a receptor truncated of its VFT domain (Binet et al., 2004; Goudet et al., 2004; Ray et al., 2005; Rovira et al., 2015) or locked by cysteine cross-links in an inactive state (Xue et al., 2015) can still be activated by agoPAMs.

1.4.2.2. 7TM domain

Based on an *in vitro* cysteine crosslinking study of the $mGlu_2$-R it was suggested that during activation, the contact interface between the protomers is changing from TM4-5 in the inactive conformation to TM6 in the active conformation (Xue et al., 2015), and only one of the protomers couples to the G-protein.

The model for activation of mGlu-Rs described by Rondard and Pin (Rondard and Pin, 2015) proposed an activation time windows of 50 milliseconds (ms) between the orthosteric ligand binding and formation of the active receptor conformation. As in family A GPCRs, an ionic lock was also identified in the crystal structures of the $mGlu_1$-R and $mGlu_5$-R between a glutamic acid in TM6 and a lysine in TM3 (Christopher et al., 2015, 2018; Doré et al., 2014; Wu et al., 2014). This ionic lock is supported by polar interaction with a serine in ICL1, and suggested to be important for activation (Doré et al., 2014). A second ionic can be found in the experimental structures of $mGlu_1$-R and $mGlu_5$-R between the glutamate in TM6 and a lysine in TM7 (Christopher et al., 2015, 2018; Doré et al., 2014; Wu et al., 2014).

No experimental structures of an active state of a family C member is available, but MD simulations of mGlu-Rs with PAMs described weakening of this ionic lock (Dalton et al., 2017), and similar effects have also been described by site directed mutagenesis (Doré et al., 2014).

1.4.3. GPCR ligands

Orthosteric compounds compete with the endogenous agonist for the binding at the orthosteric binding site. An orthosteric compound can either act as an agonist or an antagonist. When an endogenous agonist binds at the active site, the agonist stabilises the receptor in an active conformation. The magnitude of activation obtained by agonist binding depends on: the affinity for the binding site, and its efficacy. A full agonist has a high efficacy and activates the receptor to its fullest whereas a compound with less efficacy (less receptor activation capacity) than the full agonist is a partial agonist (Figure 5). Compounds that bind the receptor without triggering any effect (do not activate or turn off the constitutive activity, but has affinity), thus impairing its activation upon binding, are referred to as antagonists. An inverse agonist has a negative efficacy on the receptor activation by decreasing the constitutive activity of the receptor upon binding (Figure 5).

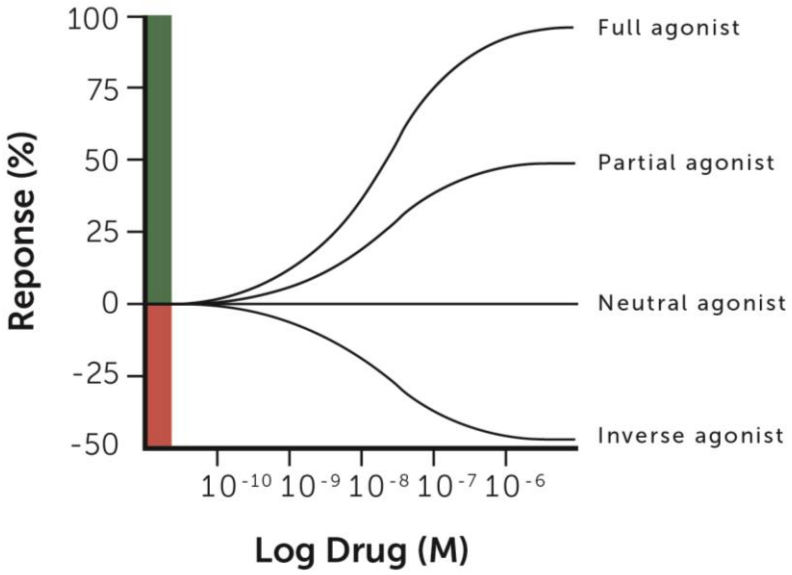

Figure 5 Dose response curve for the different type of orthosteric compounds.

AMs are ligands that bind the same target, but to a topologically different binding site than the orthosteric compounds. AMs can be of all sizes, from an ion to big chemical entities (Katritch et al., 2014). Allosteric modulation is an old concept known for at least

50 years, but has become an emerging topic in the pharmacology of GPCRs during the last years (Conn et al., 2009, 2014; Wootten et al., 2013). AMs may alter the affinity and/or efficacy of an orthosteric agonist, thus enhancing or inhibiting the receptor activation. AMs are characterized as PAMs when they increase the effects of the orthosteric agonist, or negative allosteric modulator (NAMs) when they decrease the effects of the orthosteric agonist (Figure 6). The AMs act by modulating the agonist affinity, the receptor efficacy or both, depends on the chemical properties of the AMs. In principle, the AMs act only when an agonist is present at the orthosteric site and do not trigger any effect on the receptor by itself. Nevertheless, some PAMs have been identified to have intrinsic agonist activity, and thus are called agoPAMs (Conn et al., 2014). Recently, strong agonist properties were identified for the $GABA_B$-R PAMs CGP7930 and *rac*-BHFF, and a weak activation for GS39783 without any agonist present. In the same study several specific PAMs for $GABA_B$-R were also identified (Lecat-Guillet et al., 2017).

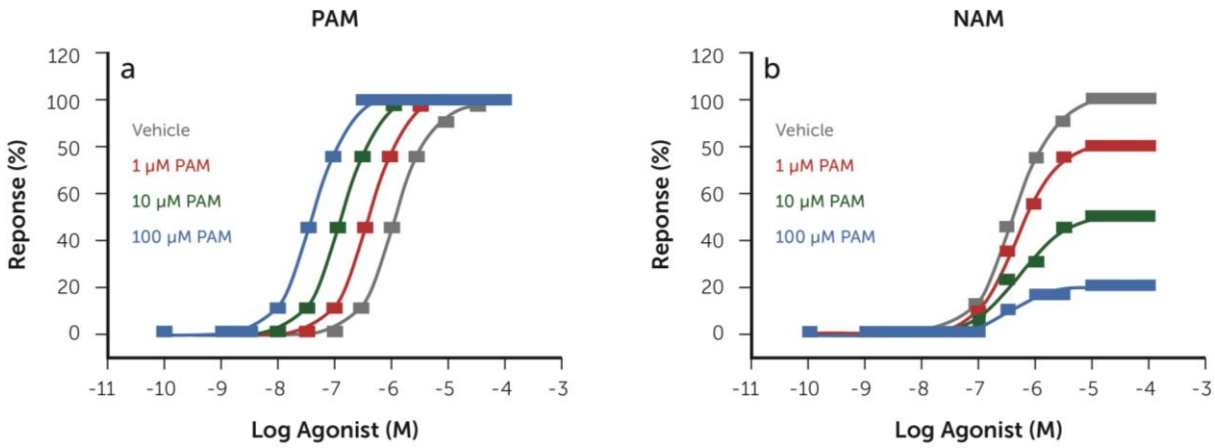

Figure 6 PAM Simple schematic representation of PAM (a) and NAM (b) activity using typical dose-response curves (modified from Niswender and Conn, 2010).

1.4.4. Allosteric GPCR modulation

In order to give a therapeutic effect, orthosteric drugs need to bind to its target. However, no compound is fully specific, and hence the ligands interact with other receptors/sites than the target. The "off-target binding" may lead to unwanted effects.

The design of subfamily specific orthosteric compounds for family A GPCRs is impaired by relative high conversation of orthosteric binding sites between family A members. Further, the high conservation of the orthosteric binding site for glutamate between the mGlu-Rs is also making the design of orthosteric mGlu-R ligands with specificity for a

particular mGlu-R very challenging (Wu et al., 2014). The allosteric binding sites are generally less conserved than the orthosteric between family members, and hence may give the opportunity to design compounds with higher specificity for the targeted receptor than the orthosteric site, and several unwanted side effects may be avoided.

Unlike orthosteric ligands, AMs do not compete with endogenous ligands for their binding site, and lower dosages may be required than for orthosteric compounds. It is therefore also less likely to develop tolerance for allosteric than for orthosteric drugs. Allosteric compounds would also give the possibility of "fine tuning" the response induced by binding of the endogenous orthosteric compound (Conn et al., 2009). In conclusion, the use of AMs as drugs may help to obtain a more specific binding, and hence lead to higher selectivity and fewer side effects. AMs cooperate with the orthosteric endogenous compound and may lead to therapeutic effect at lower dosages than traditional agonists or antagonists.

In spite of that, the design of AMs for family C members is very complex as the first experimental structures of $mGlu_1$-R and $mGlu_5$-R have been available only recently (Doré et al., 2014; Wu et al., 2014). The 3D structure of the 7TM of the $GABA_B$-R is still unknown making the design of AMs for $GABA_B$-R especially challenging. $GABA_B$-R share a sequence identity of 19% and 22% with $mGlu_1$-R and $mGlu_5$-R respectively. The difficulties are also due to possible hetero dimerization as previously described, biased signalling (see below), and that the relationships between the AM binding and the affinity/coupling efficacy of orthosteric binding site are not easy to interpret. Furthermore, some AMs for the $GABA_B$-R have been seen to be species-dependant (Sturchler et al., 2017). In addition, the exploitation of SAR data is not straightforward as small changes in the residues shaping the binding pocket or in the chemical structure of the ligand can radically changes the activity of AMs or even abolish the compound activity or change PAMs into NAMs or vice versa (for a review see Conn et al., 2014). Such changes are termed "molecular switches" and have been seen both for $mGlu_2$-R and $mGlu_5$-R (Gregory et al., 2013b; Pérez-Benito et al., 2017; Wood et al., 2011). Recently, it was suggested that these small chemical changes might have crucial impacts on the network of water molecules that is formed within the binding pocket (Christopher et al., 2018). This is also what we observe in paper 3, where we used different types of AMs complexed with $mGlu_1$-R to investigate modulator induced conformational changes on the 7TM bundle.

1.4.4.1. Family A GPCR modulators as drugs

To this date, no AMs targeting GPCRs for the treatment of brain disorders have been marketed, but long lasting efforts have brought several AMs to present ongoing clinical trials (Hauser et al., 2017). However, several marketed drugs in other disease areas are GPCR AMs, such as the drug Cinacalcet from Amgen, a specific PAM for the calcium sensing receptor, used in the treatment of hyperthyroidism (Lindberg et al., 2005) or the well-known drug Maraviroc, from Pfizer to treat HIV, is a NAM for the C-C chemokine receptor type 5 (Dorr et al., 2005).

Allosteric binding pockets have been identified within the 7TM and connecting loops of several family A receptors. In the x-ray crystal structure of the M2 muscarinic acetylcholine receptor, the allosteric compound AM LY2119620 binds within the ECLs of the 7TM bundle (pdb id 4MQT, Kruse et al., 2013). Sodium has also been identified to act as a PAM for multiple family A GPCRs (Katritch et al., 2014). The sodium binding site is found at the midrange of the receptor and displayed in the crystal structure of the adenosine receptor A2a in complex with the inhibitor ZM241385 (PDB code 4EIY, Liu et al., 2012). MK-7622, a muscarinic M1 receptor PAM developed by Merck to treat Alzheimer, was in Phase II clinical trials before the compound was stopped (Uslaner et al., 2018), and to the best of our knowledge no further testing have been performed. A list of AMs targeting GPCR of class A, B and C can be found in the supplementary data of the comprehensive review written by Conn et al. (Conn et al., 2014) as well as in the review by Hauser et al. (Hauser et al., 2017).

1.4.4.2. Allosteric modulators of $GABA_B$-receptor

It has been demonstrated that allosteric modulators of $GABA_B$-R may be pathway-dependent and species selective (Sturchler et al., 2017). It has also been shown that calcium might act as a PAM for $GABA_B$-R by binding at the VFT (Galvez et al., 2000). Only a few PAMs and a couple of NAMs are available for the $GABA_B$-R, and up to date no AMs targeting the $GABA_B$-R is marketed as a drug. However, some PAMs are in clinical trials such as the compound ADX71441 which is in phase 1 clinical trials for approval to treat Charcot-Marie-Tooth Type 1A disease (CMT1A) and alcohol and nicotine dependences (ADDEX website).

1.4.4.3. Allosteric modulators of metabotropic glutamate receptors

No endogenous AMs have been identified so far for mGlu-Rs, but numerous synthetic AMs have been developed for most mGlu-Rs (Goudet et al., 2018,) but none of them are yet in clinical use.

$mGlu_2$-R and $mGlu_5$-R are the predominant targets for drugs discovery among the mGlu-Rs, with numerous patents and several drug candidates in clinical trials, such as the specific $mGlu_5$-R NAM fenobam, which was recently solved by x-ray crystallography in complex with the $mGlu_5$-R (PDB id 6FFH, Christopher et al., 2018). This compound was discovered through a HTS campaign and was tested as an anxiolytics in the 1980s (Berry-Kravis et al., 2009) and is now tested, like mavoglurant, in a phase II clinical trial to treat Fragile X syndrome (Berry-Kravis et al., 2016). The publication of the crystal structures of the 7TM of $mGlu_1$-R and $mGlu_5$-R was a breakthrough for structure-based drug design (SBDD) of mGlu-R modulators (Doré et al., 2014; Wu et al., 2014). Chloride anions were also demonstrated to be strong PAMs for mGlu-Rs by exerting their effect at the VFT (Tora et al., 2015).

1.4.5. Biased signalling

GPCR activation leads to activation of G-proteins and/or arrestin signalling pathways and some ligand have also been identified to favour one signalling pathway over others (Rajagopal et al., 2010; Smith et al., 2018). Compounds, including some $GABA_B$-R PAMs have also been revealed to differentiate between different G-protein signalling pathways (Sturchler et al., 2017). This concept is known as functional selectivity or ligand bias (Figure 7). When a receptor in general is favouring one pathway in front of others, it is termed receptor bias, such that a ligand binding two receptors may favour G-protein coupling in one and arrestin in the other (Figure 7). The concept of biased signalling, in addition to the increased understanding of GPCR signalling pathways and disease mechanisms, may suggest that compounds with ligand bias for GPCR promoting beneficial pathways while blocking potential deleterious signals may be favourable drugs. Ligand bias increases the complexity for drug design by adding another ligand property to be refined but it also allows the design of compounds potentially more specific in relation to the disease targeted.

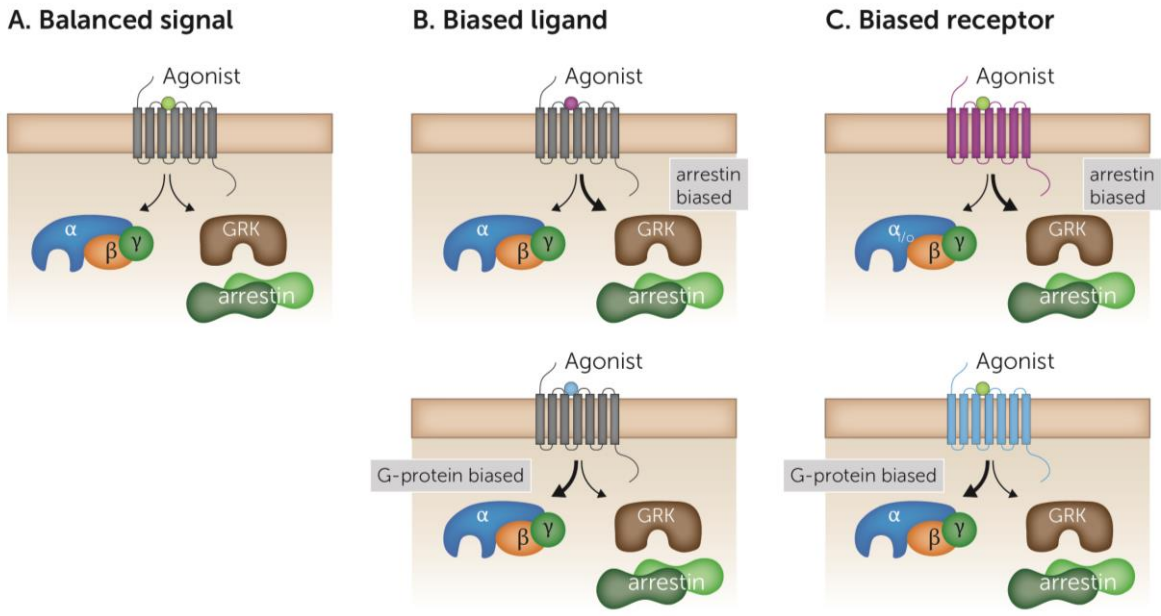

Figure 7 ***Biased signalling. A****. Balanced signalling.* ***B****. Biased ligand.* ***C.*** *Biased receptor. Purple: arrestin-biased, Blue: G protein-biased, GRK: G protein-coupled receptor kinase. (modified from Rajagopal et al., 2010)*

1.5. Molecular modelling in preclinical drug discovery

1.5.1. Modern drug discovery

A modern drug discovery process can be split into three main axes: 1.- The discovery phase, done in the laboratory with identification of the target and discovery of compounds of interest (hits), and improvements of the hits to lead compounds. 2. - Preclinical tests, performed on animals to establish the pharmacokinetics, and toxicology profiles of the compounds. 3. - Clinical trials, performed in humans to assess the efficacy, the side effects and the safety of the putative drugs (Rang et al., 2011).

The cost for bringing a new drug to the market is estimated to several billions dollars and the process can last up to 15 years (Dickson and Gagnon, 2004; Mullard, 2014). Hence, all steps in the drug discovery process need to be optimized and the use of *in silico* methods during the drug discovery campaign has become of common practice.

1.5.1.1. Drug-likeness

A drug-like compound is a compound that is sharing certain physicochemical properties with other molecules acing as drugs. The rule of five (RO5) also called Lipinski's rules of 5 were initially published in 1997 (Lipinski et al., 2001). They are a set of guidelines or strategies for designing oral drugs with good bioavailability. After

analysing marketed oral drugs and drugs validated in phase II or III of clinical trials, Lipinski came up with four properties favouring oral administration and 90 % bioavailability (good aqueous solubility and intestinal permeability): molecular weight below 500 Daltons, the logarithm of the octanol-water partition coefficient (log P) <5, no more than 5 hydrogen bond donors and a maximum of 10 H-bond acceptors. If the compound of interest is breaking more than one of these rules, it most likely has low bioavailability after oral administration.

For CNS drugs, others parameters such as their capacity to pass the blood–brain barrier (BBB) and their affinity for transporter proteins found in the BBB need to be taken into account. Hence, a compound satisfying the Lipinski rules and in addition has a total number of oxygen plus nitrogen atoms < 5 (Norinder and Haeberlein, 2002) might have good BBB penetration, and if the drug in addition has a polar surface area (PSA) < 60-70 (Kelder et al., 1999) or a log *P* – (N+O) > 0 (Norinder and Haeberlein, 2002), the compound most likely penetrates BBB and may be CNS active.

The RO5 filtering is usually one of the first steps done to reduce the number of compounds from a chemical database during drug development but the administrative route of the drug should also be considered. The chemical space of putative "drug-like compounds" was estimated to be between 10^{23} and 10^{60} molecules (Polishchuk et al., 2013) while there are more than 20,000 proteins in the human genome. Thus, the use of screening techniques is necessary for a fast identification of hit compounds for a given target protein as the number of potential compound-protein associations is very huge.

The screening can be performed *in vitro* by high-throughput screening (HTS) techniques. HTS requires the design of fast and sensible techniques. The quite small numbers of compounds that can be tested in a short amount of time and the cost associated limit the use of HTS as the initial screening in drug discovery campaigns (Hawkins and Stahl, 2018). *In silico* methods can be used to handle massive amounts of data in a short time and require less resources than traditional *in vitro* methods. This makes such approach a suitable alternative for initial screening in the first stage of a drug discovery campaign. These methods are often termed as computer-aided drug design (CADD).

1.5.2. Molecular mechanics and force fields

"Molecular modelling encompasses all theoretical methods and computational techniques used to mimic and study the structure and behaviour of molecules, ranging from small chemical systems to large biological molecules and material assemblies." (definition from https://www.nature.com/subjects/molecular-modelling). During the last decades, molecular modelling has evolved with the increase of central processing unit (CPU) power, and is today commonly used in drug discovery to:

- Quick identification of hit compounds (screening)
- Identify ligand structures that can be obtained from suppliers or synthesised
- Improve a hit into a lead compound
- Predict the activity/toxicity of a chemical compound
- Analyse protein-ligand interactions through docking and molecular dynamics (MD) simulations (also applicable for protein-protein interactions)
- Find structurally similar compounds
- Generate pharmacophore models, structure–activity relationship (SAR), fingerprinting, and other ligand-based methods.

The description of molecules is done using mathematical terms. According to the aim of the calculations and size of the molecular system different approaches are used to describe the system: quantum mechanics (QM), molecular mechanics (MM) or a hybrid method using both (QM/MM). In QM, molecules are described at the atomic scale with each subatomic particle considered as individual entities. In MM, the movements of electrons are ignored. Hence, each atom composing the molecular system is described as spheres linked to the others by springs (Höltje, 2008). The spheres are centred on the nucleus with a volume corresponding to their van der Walls (vdW) radius. The springs represent the bonded interaction (covalent bonds) and the electrons are non-described.

An *in silico* description of a full protein by QM is currently not possible due to large CPU demands (Bordner, 2012). On the other hand, it is possible to use a hybrid QM/MM approach to evaluate the contribution of residues or water molecules involved in the protein-ligand interactions or to study a chemical reaction (Gräter and Li, 2015). In a hybrid QM/MM approach, the binding site and the ligand are described using QM, while the remaining part of the system is described by MM. MM is more commonly employed

to describe large biological system like protein complexes, having a balance between the accuracy of the description and CPU costs.

In MM, the total energy function, or the potential energy function, links the geometry of a molecular system to its energy (Bordner, 2012). The total energy (E_{tot}) of a system is calculated by summing the different forces involved in the covalent interactions of the system (E_{bonded}) and the interactions between all pairs of atoms not bonded chemically ($E_{non\text{-}bonded,}$). E_{bonded} is the sum of the energy terms expressing bond- stretching and -compressing (E_{bond}), angle bending (E_{angle}) and torsion ($E_{dihedral}$). $E_{non\text{-}bonded}$ is the sum of the energy terms representing the electrostatic ($E_{electrostatic}$) and van der Waals (E_{vdW}) interactions (Bordner, 2012) . The total energy of the molecular system can be written as (equation 1):

$$E_{tot} = E_{bonded} + E_{non\text{-}bonded}$$
$$E_{bonded} = E_{bond} + E_{angle} + E_{dihedral} \quad \textbf{(1)}$$
$$E_{non\text{-}bonded} = E_{vdW} + E_{electrostatic}$$

The different terms of the potential energy function are usually described as harmonic potentials with optimal values (reference values) calculated or obtained from *ab initio* quantum calculations and experimental data (Bordner, 2012). The collection of the unstrained values together with empirically derived parameters (the force constants) are called force fields (Lindahl, 2015). A deviation from the reference value (positively or negatively) results in an energy penalty. The form of the potential energy function and the optimal values in the parameter file can vary between force fields depending for what they are designed for (Bordner, 2012). One geometry of the molecular system is associated with one E_{tot} and by mapping all the E_{tot} a system can take; a landscape of potential energy can be drawn (Figure 8) with only one global minima (in blue on the figure) and several local minima.

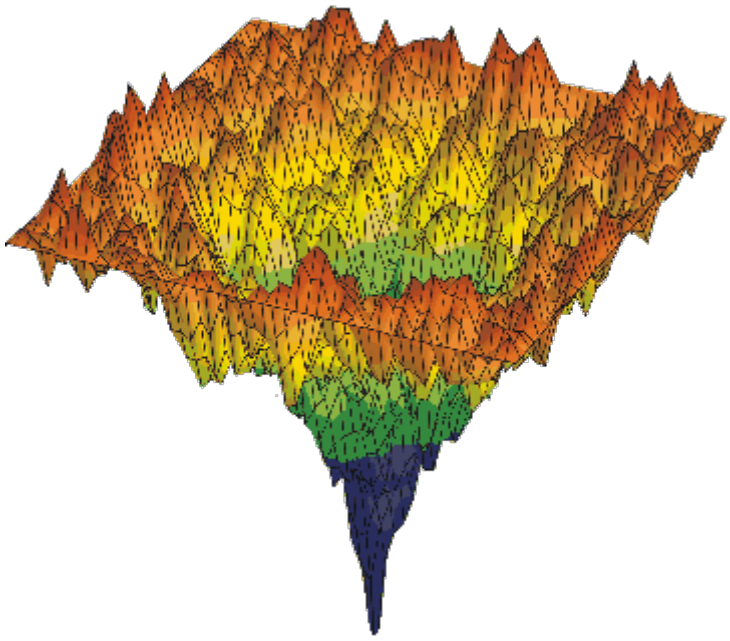

Figure 8 *Illustration of a landscape of total potential energy for a given protein with multiple local minima and one global minima (from http://www1.lsbu.ac.uk/water/images/dry_surface.gif).*

1.5.3. Molecular modelling techniques

As previously mentioned, the number of putative compounds with drug-like properties is very huge, and hence, *in silico* screening techniques are used to rapidly discriminate inactive compounds from those susceptible to be active. Compounds predicted *in silico* as highly active are further tested by experimental methods. These *in silico* steps are referred to as Virtual screening (VS), which can be considered as the *in silico* parallel to HTS.

VS methods can be divided into two main approaches: structure-based and ligand-based VS methods (Cross, 2018). The structure-based methods can be employed when the structure of the target protein is known at the atomic level. That can be 3D structures obtained by experimental methods (x-ray crystallography, Nuclear Magnetic Resonance, sometimes also cryo-EM) or by homology modelling. Ligand-based methods can be employed when we have information about known active ligands for the target protein. In the studies that the thesis is based upon, we have utilized a combination of both methods. Homology modelling technique is considered as structure-based method as it uses knowledge about the 3D structure of homologous proteins as templates. In the following, I will explain in more detail the *in silico* methods that have been used during the PhD project.

1.5.3.1. Databases

Independent of the VS approach used for the identification of new compounds, a critical point is the choice of compound database for the screening. A chemical database for screening can contain several million compounds. The compounds can be of all origin, natural products, stable theoretical compounds (Ruddigkeit et al., 2012), or commercially available synthetic compounds. Chemical databases can be from commercial vendors, academic, private (pharmaceutical companies), and be general or more focused libraries of compounds. A typical updated database might contain from thousand up to several million diverse compounds, and hence, it is essential to handle the database with care. The databases should be pre-optimized to:

- Remove duplicates
- Eliminate extra chemical entities, like ions or solvent from the compound of interest
- Check correct representation (3D) of the compounds.
- Only keep compounds compatible with the aims of the project

1.5.3.2. Ligand-based methods

1.5.3.2.1. Fingerprinting

Ligand-based methods use information from the structure of known ligands for the target protein to identify new compounds (Wishart, 2015). Both 2D and 3D ligand-based methods can be employed. Binary fingerprinting is a 2D ligand-based method (Cereto-Massagué et al., 2015; Hawkins and Stahl, 2018). The chemical structure of a set of known target binders can be described by binary fingerprints (bit strings, Figure 9). These fingerprints are then used to screen *in silico* databases to identify compounds containing similar binary fingerprints, with the aim of retrieving putative new ligands for the target protein (Willett, 2006).

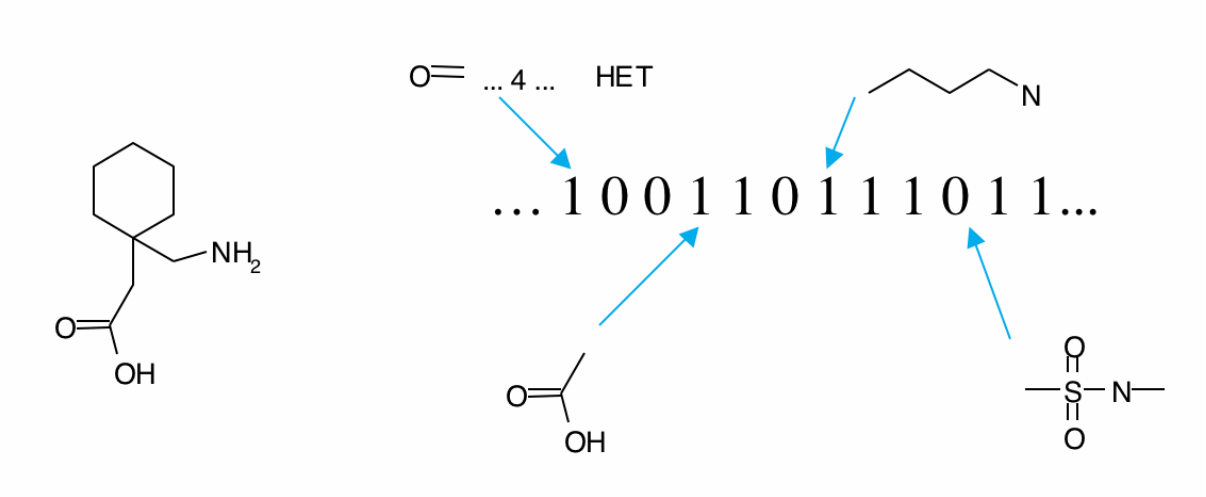

Figure 9 Binary fingerprint. *Illustration of binary fingerprints. Each chemical moiety of the molecule will activate a specific bit. At the end, the molecule is described as a string of 0 and 1 where 1 indicates presence of a chemical moiety, while 0 indicates that the moiety is not present. https://i571.wikispaces.com/file/view/Picture_18.gif*

Multiple types of fingerprints exist to describe chemical features, and several should be tested to identify the best for a particular set of compounds (Duan et al., 2010). Once the type of fingerprint is selected, a similarity search is performed in the chemical database to retrieve similar compounds using similarity metrics like the Tanimoto coefficient (Tc, equation 2, Cereto-Massagué et al., 2015). Tc is a value between 0 and 1 with 0 indicating the two compounds are completely dissimilar, while 1 indicate that the compounds are identical.

$$\boldsymbol{Tc = \frac{c}{a+b-c}} \quad \textbf{(2)}$$

In equation 2, a is the number of bits activated in compound A, and b the number of bits activated in compound B. C is the number of common activated bits for molecule A and B.

1.5.3.3. Pharmacophore modelling

Ligand-based 3D pharmacophore models are representations of the 3D structural features necessary for activity among a group of known active compounds (Horvath, 2010), while structure-based pharmacophore models are generated based on protein–ligand complexes from experimental studies or docking. Structure-based and ligand-based pharmacophore models express the set of chemical features (hydrogen bonds

donor/acceptor, hydrophobic, etc,) a ligand (active or inactive) should possess or not in order to obtain activity for the target protein (Figure 10).

The building of ligand-based pharmacophores is done by generating and aligning conformations of the known compounds in order to identify the crucial chemical functions needed for activity (Horvath, 2010). Several pharmacophore models can be generated from the same set of ligands, and their quality is assessed using scoring metrics such as the Youden index (Youden, 1950) that was used in paper 2. The selected pharmacophore models (ligand-based or structure-based) are then used to screen a database to retrieve compounds that match with the models (Labute, 2018).

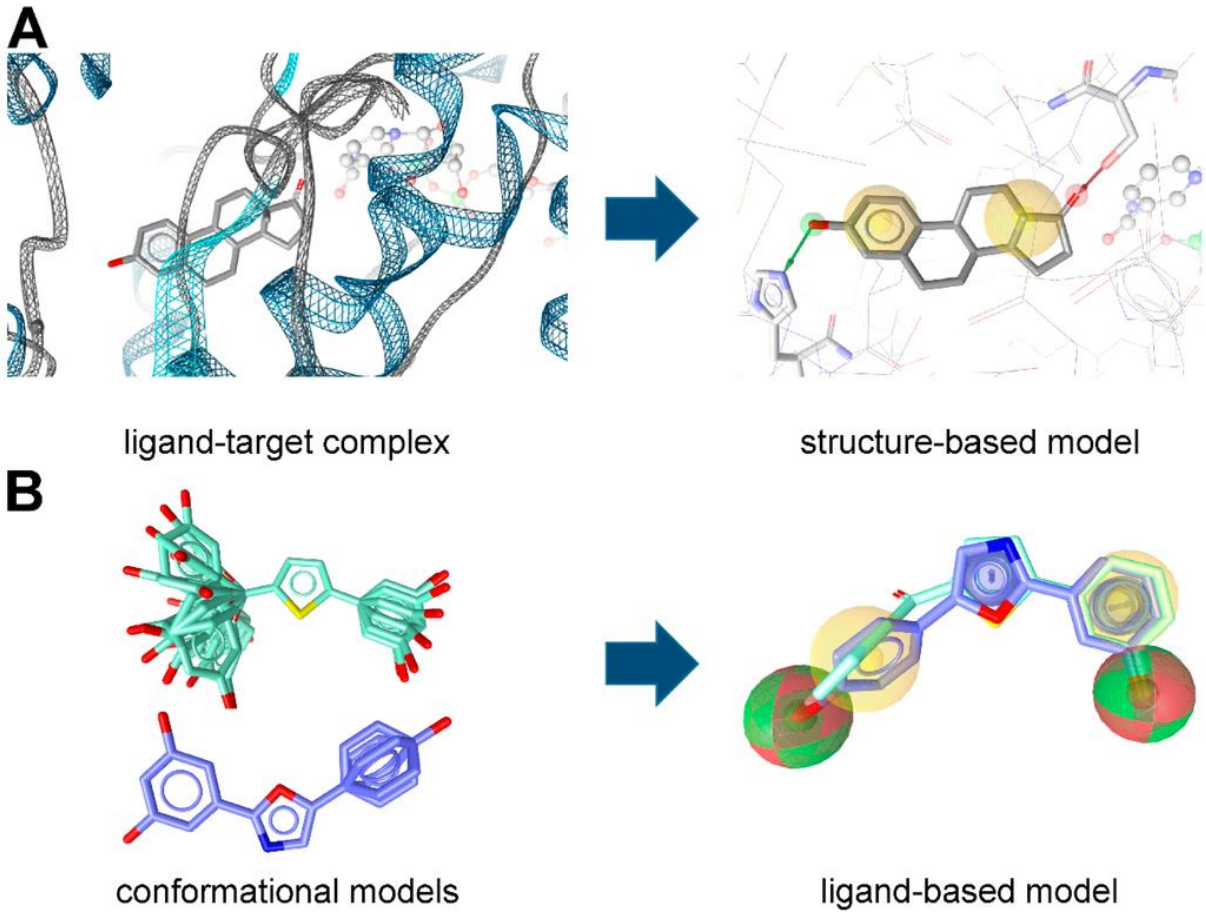

Figure 10 Pharmacophore models. *Illustration of a structure-based (**A**) and a ligand-based (**B**) pharmacophore models with the definition of different chemical features found in the ligand(s)- Yellow spheres: hydrophobic, red spheres hydrogen bonds donor and green sphere: hydrogen bonds acceptor. (Kaserer et al., 2015)*

1.5.3.4. Structure-based methods

1.5.3.4.1. Homology modelling

When the atomic resolution 3D structure of the target protein is unknown, computational methods can be used to predict the 3D structure. Several molecular modelling methods are available for structural predictions including *ab initio* and homology modelling techniques. The most used method for such predictions is homology modelling, where the 3D structure of a homologues protein (template structure) is used as a starting point to construct a theoretical 3D model of the target protein. This technique is possible due to a higher conservation of the 3D structure than the sequence (Chothia and Lesk, 1986). The evolution of secondary structures is also slower than of loops, hence secondary structures are more conserved than loops between homologue proteins. In order to construct reliable models, it is important that a template structure with appropriate amino acid sequence homology and related function to our target is available. Thus, every new experimental structure is not only a success for the subfamily the solved protein belongs to but also for all its structural homologues. It is generally believed that a sequence identity of at least 30 % between the template and target is necessary to obtain reliable models of membrane proteins (Forrest et al., 2006). Structural experimental studies of membrane proteins are not straight forward and the number of GPCR structures with known 3D structure is still quite limited (Pándy-Szekeres et al., 2018), although it has been a huge increase in the number of available GPCR structures during recent years (Cvicek et al., 2016). For each solved GPCR structure, the number of GPCR members that can be predicted by homology modelling is also increasing.

The homology modelling method contains several steps (Figure 11) (Simms, 2010);

1. **Template identification**: A blast search is performed with the sequence of the target protein against structures in the PDB databank. Usually, the 3D structure(s) with the highest sequence identity with the target will be selected as template(s).

2. **Template-target alignment**: the sequence of the target protein and the sequence extracted from the crystal structure of the template are aligned. The sequence alignment is a critical step; the conserved residues need to be correctly aligned to generate reliable models. To identify conserved residues a multiple sequence alignment (MSA) is usually constructed.

3. Model building: This is the step where the theoretical 3D model of the target protein is built. The conformations of conserved amino acids are copied from the template, while the conformations of non-conserved amino acids are built or generated by searching rotamer libraries. Due to high structural flexibility, some loops are often lacking in the experimental 3D template structures, and these missing parts need to be generate by *ab-initio* or knowledge-based approaches.

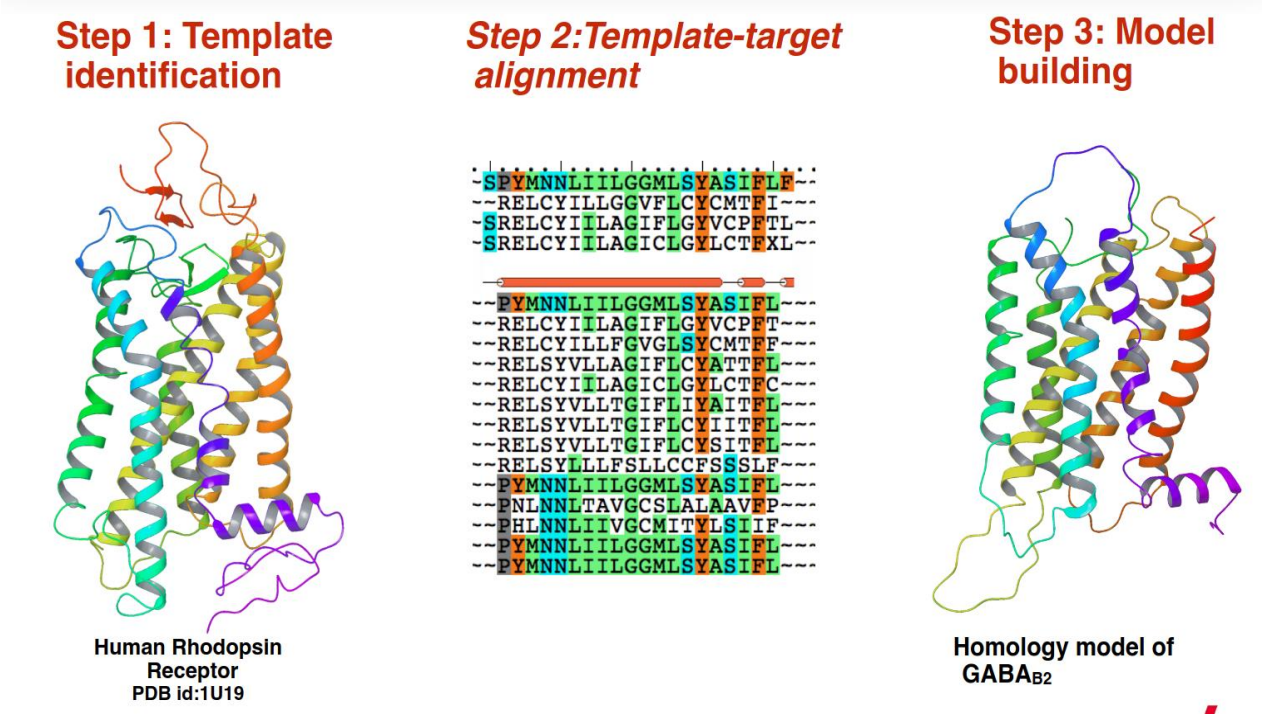

Figure 11 Homology modelling steps. *Schematic representation of the main steps for building a theoretical 3D model of a protein.*

1.5.3.4.2. Docking and scoring

When a detailed 3D structure of the target protein is available from experimental studies or homology modelling, it is possible to predict the binding orientation (docking pose) of a ligand in the binding pocket of the target protein (Figure 12). The docking approach is commonly used in drug discovery to predict putative binders from a set of compounds , to split between true ligand (true positive) and decoys (true negative), and to rank between a set of compounds (Sliwoski et al., 2014).

The docking procedure consists of two steps: 1) a search algorithm that explores different binding poses of the ligands inside the binding pocket of the protein 2) a scoring function that predicts the strength of the protein-ligand interactions of the docking pose.

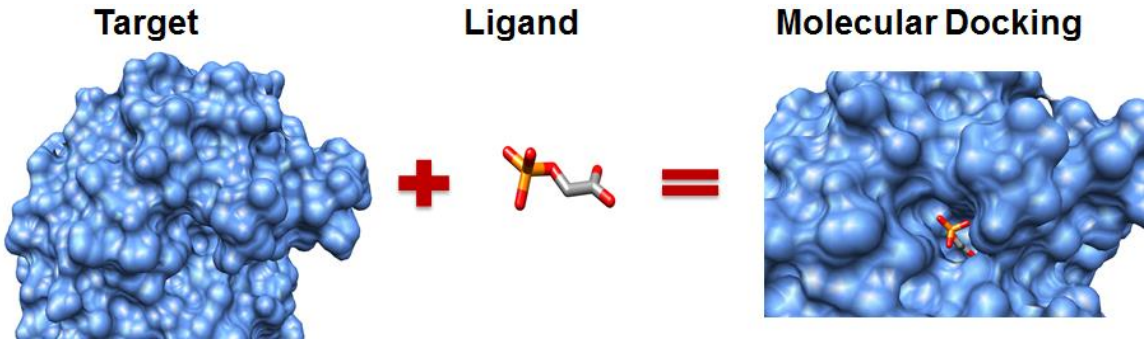

Figure 12 Docking. *Illustration of the docking procedure (Tenorio et al., 2013)*

The binding of a ligand to a protein was described by the "key-lock principle", but today we know that this is a dynamics process where both the ligand and the protein undergo conformational changes adopting to the structure of each other (Vogt and Di Cera, 2013). The previous and the present concepts are reflected in the different approaches of docking available: Rigid and semi-flexible docking. The computation of the ligand and protein flexibility increases the time and CPU cost for the process.

In rigid docking, both the compounds and the protein are kept rigid. Hence, the only degree of freedom for the compounds within the binding pocket is rotation and translation. Such approach is very fast and allow the screening of databases of millions of compounds. The flexibility of the ligand in rigid docking can be taken into account by prior generation of ligand conformations. A more CPU costly method adds another degree of freedom to the ligands, the torsion. This is the default procedure for docking with the software Glide (Friesner et al., 2004). The ligand is fully flexible while the protein is kept rigid. Docking methods that encompasses flexibility of both the protein and ligand (flexible docking) have also been developed and is implemented in several docking programs (Lexa and Carlson, 2012). However, it is still too computationally intensive (Lexa and Carlson, 2012) to be the default procedure for SBDD.

The 3D geometry of proteins in x-ray crystal structure reflects the most populated conformation during the crystallization. As mentioned above, the binding pocket of a protein adapts to its ligand. Hence, if a crystal structure was solved with a ligand, the binding pocket conformation might not be ideal for optimal docking results of even close ligand analogues if the protein is kept fully rigid. *In silico* methods may be used to explore alternative proteins conformations, including induced fit docking (paper 1), Monte-Carlo and MD simulations (see below and paper 3). Monte-Carlo simulation is a stochastic process independent to time, contrary to MD simulation. Further, the protein flexibility

can also be taken into account by docking the same set of ligands to several conformations of the binding pocket (Gabrielsen et al., 2012, paper 1, paper 2).

Scoring functions are used to rank different docking poses by assigning a score value to the poses, which reflects a predicted *in silico* affinity. This step is also important since wrong evaluation of poses leads to a wrong selection of ligands for further testing. Hence scoring functions help to discriminate "real" ligands (true positive) for the target protein among numerous other ligands but can also help to determine the correct binding pose when several docking poses are proposed for a same ligand (Orry and Abagyan, 2011).

The evaluation of a docking pose is performed by calculating its absolute binding energy for the protein target by resolving the free energy of binding (ΔG) given by the Gibbs Helmholtz equation (equation 3) with ΔH as the enthalpy change, T the temperature, ΔS the entropy change, R the gas constant and K_{eq} the equilibrium constant. The ΔG calculations are CPU demanding, and hence approximations are used to increase the output speed.

$$\Delta G = \Delta H - T\Delta S = -RT \ln K_{eq} \quad \textbf{(3)}$$

Prior to docking, the location of the ligand binding site in the protein need to be determined based on knowledge about the binding pose from 3D structure complexes, or for example from site directed mutagenesis data. Ligand QSAR data may also guide in the determination of the binding site. Then the docking grid has to be calculated. Each grid point represents the physicochemical properties of the binding site. The docking software then fits the ligand into the grid points to generate the optimal ligand-protein binding (Friesner et al., 2004).

1.5.3.4.3. Molecular dynamics simulations

The aim of molecular dynamics (MD) simulation is to mimic protein motions *in silico* over time. MD simulations are computationally very costly, and the protein motions are usually only studied for time periods of nanoseconds (ns) to microseconds (µs)(Lindahl, 2015). However, the increasing power of calculation available open new perspectives of longer time scales of simulations, especially with the general-purpose graphic processing unit (GPGPU) calculations (Loukatou et al., 2014) or dedicated hardware like the Anton supercomputer (Shaw et al., 2008). MD simulations also use force fields to compute the

energy of the molecular system as a function of geometry, although MD simulations using QM (Nurisso et al., 2011) or hybrid combination of QM/MM are also available. The interacting forces are calculated from the potential energy expression and the atoms are treated as particles that move in accordance with Newton's second law (Lindahl, 2015) also called the equation of motion (equation 4).

$$F_i = m_i a_i = m_i \frac{d^2 r_i(t)}{dt^2} \quad \textbf{(4)}$$

The ensemble of forces applied on particles, $\mathbf{F_i}$, is equal to the product of the masse of the particles, $\mathbf{m_i}$, by their acceleration, $\mathbf{a_i}$. The particles represent atoms composing the molecular system. The acceleration is the second derivative of the position of a particle with respect to time.

By knowing the position of the particle and the velocity vectors it is possible to describe the evolution of the molecular system over time and to draw an MD trajectory. This is done by integrating the equation for each time steps, Δt. The time step should not be longer than the fastest movements in the molecular system, otherwise it would lead to unreliable simulations (bonds vibration: 10^{-14}-10^{-13} second). However, if the time step is too small, the simulation will be too computationally demanding. Usually the time step is in the time scale of 1-2 fs (Lindahl, 2015).

MD simulation of proteins need to pass several steps in order to obtain a stable distribution of energy (velocity) throughout the molecular system before the "production" phase can start (Nurisso et al., 2011). The production phase is then used to analyse the protein motions and protein-ligand interactions.

The different steps in an MD of a membrane protein can be as follows (paper 3): 1. - Preparation of the protein/complex: adding of hydrogen atoms and removal of steric clashes. 2. – Embedding the system into a dual lipid membrane layer (the choice of the lipid depends of the purpose of the study and the temperature used for the MD). 3. - Neutralization of the molecular system with counter ions. NaCl can be added to mimic natural settings. The system is solvated with water molecules (Figure 13) 5. - Relaxing the molecular system and heating to the desired running temperature. 6. - The production run.

During the relaxation phase, putative constraints applied on different components of the system are released step by step, usually followed by a few ns of unconstrained MD

before the production phase. One of the crucial steps is the distribution of velocity, which will affect the initial direction the simulation will take.

After the recent success of several studies (see examples Dalton et al., 2017), MD simulation has turned to be an well accepted tool and its applicability is well established, also for membrane proteins (Miao and McCammon, 2016; Velgy et al., 2018). For instance, using the especially designed supercomputer Anton (Shaw et al., 2008), activation of the β2 adrenergic receptor was simulated (Dror et al., 2011). MD simulation can be used to study time-dependent protein-ligand interactions, the binding/unbinding of a ligand with a target (Marino and Filizola, 2018), protein folding, study the binding mode of a ligand or family of ligands in order to improve their structure or to generate mutated target to validate generated hypothesis (Carlsson and Persson, 2011).

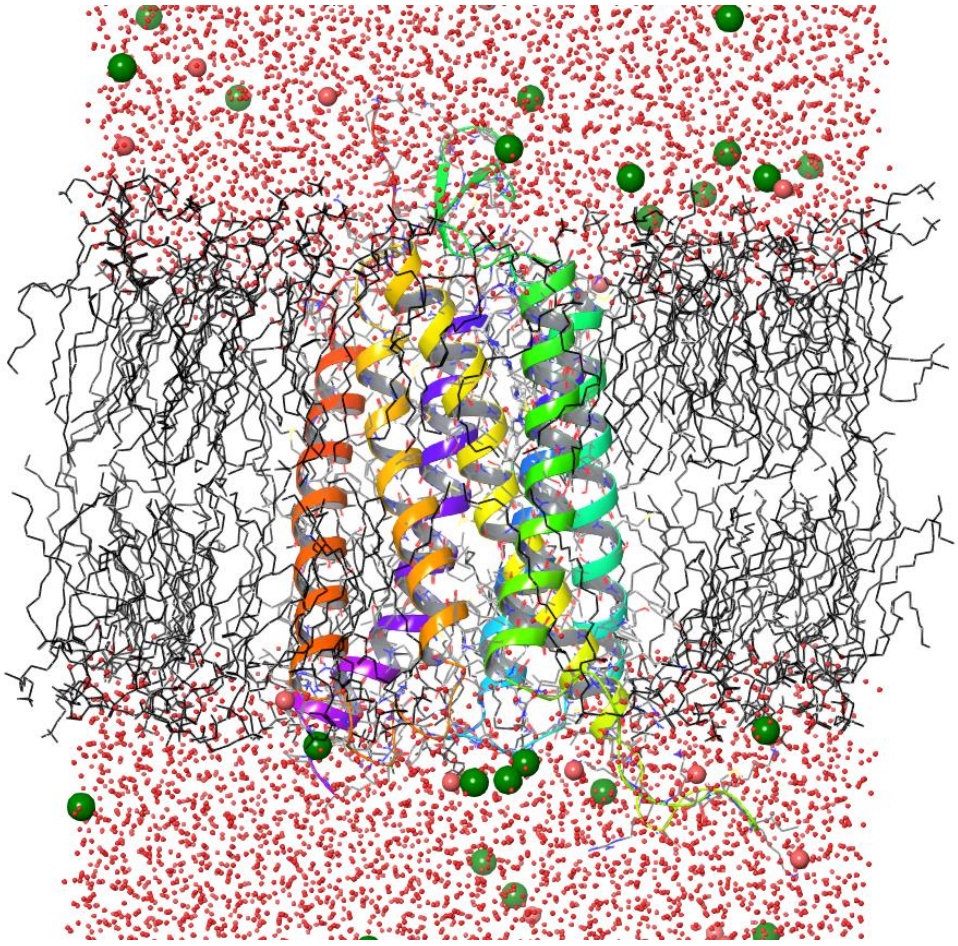

Figure 13 : ***MD system.*** *Illustration of a prepared MD simulation complex of a membrane protein. Crystal structure of mGlu$_1$-R in complex with the ligand FITM (rainbow color, PDB code 4OR2, (Wu et al., 2014)) imbedded in a dual lipid membrane (in black) with chloride (green spheres) and sodium (red spheres), and solvated in water (red dots).*

2. Aim of the study

As described in the introduction, GPCRs are involved in numerous physiological processes and diseases. Approximately one third of present drugs target GPCRs. Traditional drugs are orthosteric ligands and may be associated with numerous non-wanted effect due to off-target interactions. Allosteric modulators have several advantages in front of traditional agonists and antagonists, and allosteric binding sites have been identified in both the $GABA_B$-R and the mGlu-Rs.

Allosteric modulators of the $GABA_B$-R may have a huge potential as drug candidates in several disease areas, few PAMs are already known, but only a couple of NAMs. VS combined with experimental *in vitro* studies have gained success in identifying hit compounds that can be developed into lead candidates for drug discovery (Ripphausen et al., 2010). The 3D structure of the 7TM domain of $GABA_{B2}$-R subunit has not been resolved experimentally. In order to screen for new allosteric ligand candidates by combining *in silico* and *in vitro* studies we need a structural model of the $GABA_{B2}$-R subunit.

The molecular mechanisms of allosteric modulation are not well understood, especially for family C GPCRs. It is not clear how the binding of an allosteric modulator can induce conformational changes leading to positive or negative allosteric modulation. MD simulations can be used to study induced conformational changes of proteins upon ligand binding and may help to gain insight into the allosteric binding process.

The particular aims of the present study were therefore:

- Generate homology models of the transmembrane domain of the $GABA_{B2}$-R containing the allosteric binding site with conformations compatible with the known active PAMs
- Propose amino acids of the $GABA_B$-R involved in binding of AMs
- Establish a combined ligand-based and-target based VS approach that is using the $GABA_{B2}$-R models to screen filtered databases of commercial vendors to identify and select putative new AMs for further *in vitro* characterization.
- Study the impact of the binding of different AMs on the conformation and dynamics of the crystal structure of $mGlu_1$-R with non-biased MD simulations.

3. In silico methods in the studies

3.1. Software choices

3.1.1. Paper 1

The Modeller software (Fiser and Šali, 2003) was employed to generate $GABA_{B2}$ –R models. The induced-fit docking was performed using with the Schrödinger Induced Fit Docking (IFD) protocol (Small-Molecule Drug Discovery Suite 2014-1: Schrödinger Suite 2014-1). The different 3D structures of $GABA_{B2}$-R models were prepared with the one-step protein preparation workflow in Schrödinger Maestro. The clustering of the PAMs was handle using Schrodinger Canvas software (Schrödinger Release 2014-1:). Docking of the PAMs was performed using the Schrödinger Virtual Screening Workflow (VSW) tool with the Glide Standard Precision (SP) method (Small-Molecule Drug Discovery Suite 2014-1:) and the OPLS2005 force field (Banks et al., 2005). The evaluation of the ligand specificity of the different $GABA_{B2}$-R models was done using the Boltzmann-enhanced discrimination of receiver operating characteristic (BEDROC) method (Truchon and Bayly, 2007). The protein-ligand interaction analysis was done using in-house scripts of Structural Interaction Fingerprints (SIFt, Mordalski et al., 2011).

3.1.2. Paper 2

ADMET filtering of the assembled database was performed using Schrödinger Qikprop (Schrödinger Release 2014-1:). Pharmacophore models were generated with the Phase software from the Schrodinger Suite (Schrödinger Release 2014-1:). The conformations were sampled using the software ConfGen (Schrödinger Release 2016-1:) The structure-based VS workflow was handled using the VSW tool from the Schrodinger Suite with SP methods (Schrödinger Release 2016-1:). The scoring of the docking poses of the screened ligand was calculated with Prime (Schrödinger Release 2016-1:) and the MM-GBSA approach (Li et al., 2011). The clustering and fingerprint of the output were performed with the Canvas software (Schrödinger Release 2016-1:).

3.1.3. Paper 3:

The $mGlu_1$-R:NAM complex was obtained from the x-ray crystal structure of $mGlu_1$-R co-crystalized with FITM (PDB code 4OR2, Doré et al., 2014)). The missing loops in the $mGlu_1$-R x-ray crystal structure were built using Schrödinger Prime (Schrödinger Release 2016-4:). The PAM and agoPAM selected for running the MD simulation were prepared with LigPrep (Schrödinger Release 2016-4:). The docking was performed with

Schrödinger Glide software (Schrödinger Release 2016-4:) and score using Prime and the MM-GBSA approach (Schrödinger Release 2016-4:). The MD simulations were performed using Desmond (Schrödinger Release 2016-3:) with the OPLS3 force field (Harder et al., 2016). Analysis of MD trajectories was performed with the module "simulation interaction diagram" (SID) in Maestro. Visual Molecular Dynamics 1.9.3 (VMD) developed by the Theoretical and Computational Biophysics group at the University of Illinois at Urbana-Champaign (http://www.ks.uiuc.edu/Research/vmd/) was employed to analyse interhelical hydrogen bonds and the ionic interactions during MD simulations. The analysis of hydration points was performed by using a script developed by Johann Hendrickx (https://gitlab.univ-nantes.fr/hendrickx-j/protein_hydration_sites.git).

3.2. Alignment and homology modelling (paper 1)

A published alignment between the $mGlu_1$-R and the human CXCR4 receptor (PDB ID: 3ODU as well as other family C GPCRs (Wu et al., 2014) was used as initial alignment for constructing the homology models. The templates sequences and the $GABA_{B2}$ sequence were added and manual adjustments performed. The homology modelling technique was chosen over *ab initio* for the building of the 3D models of $GABA_{B2}$ subunit due to the availability of templates. Furthermore, the variety function of MODELLER was used to build models with different conformations to scan the conformational space of $GABA_{B2}$. The numbers of generated models from each template were set to 100 due to the capacity of the VSW module to handle 100 different receptors maximum in one run.

The evaluation of the models to enrich known active compounds against decoys is a common procedure and has been used with success in other complicated modelling projects (Carlsson et al., 2011; Kufareva et al., 2014; Phatak et al., 2010; Rodríguez et al., 2014). To refine the models and decrease the bias inherited from the templates, additional conformations of the models were generated by IFD.

3.3. Virtual Ligand Screening

The Virtual Screening Workflow of the Schrodinger Suite was used for the multistep docking and ranking procedure. A database was assembled by merging 5 commercial datasets of ligands. Before the *in silico* VS, the database had to be filtered. Hence, an ADMET filtering was performed using physicochemical parameters derived from the

known actives followed by a pharmacophore mapping. One pharmacophore model was generated for each cluster of known PAMs selective for $GABA_{B2}$-R.

After the ligand-based approaches, the database was docked into the eight selected $GABA_{B2}$-R models from paper 1, each of them specific for only one cluster of PAMs.

3.4. Molecular dynamics simulations

In order to create the $mGlu_1$-R:PAM and $mGlu_1$-R:agoPAM complexes, both ligands were docked into the crystal structure of $mGlu_1$-R (PDB code 4OR2, Doré et al., 2014)) while the $mGlu_1$-R:NAM complex was from the PDB-database (PDB code 4OR2, Doré et al., 2014)).

Non-biased MD simulations were run on GPU to access the μs timescale of simulation with a reasonable amount of computational time. During the simulations, Nosé–Hoover–Langevin dynamics were used to simulate the NPT ensemble, in which the number of atoms (N), the pressure (P) and temperature (T) were fixed with T = 310 K, and P = 1.01325 bar. To orient the complexes in the membrane, all inputs were superimposed with the pre-orientated $mGlu_1$-R structure from the Orientations of Proteins in Membranes (OPM) database (Lomize et al., 2006). The TIP3P water model from the OPLS3 force field was used as the solvent and the systems were neutralized using Cl- and Na+ as counter ions and 0.15M NaCl were added.

4. Summary of results

4.1. Paper 1

Freyd, T., Warszycki, D., Mordalski, S., Bojarski, A.J., Sylte, I and Gabrielsen, M (2017) **Ligand-guided homology modelling of the $GABA_{B2}$ subunit of the $GABA_B$ receptor**. *PLoS One, DOI 10.1371/journal.pone.0173889*

All known PAMs for $GABA_B$-R were retrieved from the scientific literature and clustered into 5 structural clusters. Using 6 templates from GPCR families A, B and C, 600 crude homology models were built. The initial models were then ranked by their capacity to discriminate the clusters of known PAMs from property matched decoys. Additional 500 models were generated using the IFD techniques and tested like the first 600 models. After evaluation, 8 models were selected based on their specificity for the different clusters of known PAMs. No models were found specific for cluster 3 of PAMs, but cluster 3 shown good binding for some of the other models. Unambiguously, the models based on the family C templates were the best to enrich known PAMs.

By analysing the protein-ligand interactions of the selected models with their specific clusters of PAMs, 24 residues belonging to TM3-5-6-7 were identified to shape the putative PAM allosteric binding site of $GABA_{B2}$-R. The putative allosteric binding pocket identified in $GABA_{B2}$ is rather hydrophobic like in $mGlu_1$-R and $mGlu_5$-R and several residues were conserved within the $mGlu_{1-8}$-R allosteric binding sites.

9 residues were proposed as hot spots as they were in range of interaction with the known PAMs in more than 95 % of the docking experiments in the eight selected $GABA_{B2}$ models. Out of the 9 residues, 8 correspond to positions that were found to be involved in AM binding in other family C members (Pándy-Szekeres et al., 2018). Some of the hot spots identified for the $GABA_{B2}$-R PAMs were located at positions with low conservation among mGlu-Rs (Doré et al., 2014).

4.2. Paper 2

Freyd, T., Wushur, I., Evenseth, L.M., Warszycki, D.,, Brandski P., Pilc, A., Bojarski, A.J., Gabrielsen, M. and Sylte, I. (2018) **A virtual ligand screening approach for new $GABA_B$ receptor modulators.** *Manuscript*.

Using the $GABA_{B2}$-R models from paper 1, a VS campaign was established to identify putative $GABA_B$-R AMs. A database of 8.2 million compounds was assembled by merging the databases of 5 commercial vendors. Ligand-based methods were employed for a

multistep filtering. ADMET filtering was performed followed by 3D pharmacophore filtering of the database. Pharmacophore models were generated for each of the 5 clusters of known PAMs (paper 1). The ligand-based approach decreased the number of compounds from 8.2 million compounds to 8021 unique compounds.

The remaining compounds were docked into the 8 selected homology models from paper 1. After docking, a final step of MM-GBSA calculation was performed on the top 10% of the docking poses. After MM-GBSA, the 20 best scoring compounds in each of the 8 $GABA_{B2}$-models were considered for visual inspection and following selection for purchasing. In the selection, their 3D structure, structural similarity with known PAMs (paper 1), ranking after MM-GBSA and their binding pose were taken into account, and 55 ligands were purchased for experimental validation. A functional assay studying the generation of cAMP was established and the effect of the purchased compounds in modulating the cAMP response was studied using Chinese hamster ovary (CHO) cells overexpressing the $GABA_B$-R (B1a/B2) and native CHO cells. Out of the purchased compounds, experimental studies identified 3 putative PAMs (compounds 35, 38 and TI400), and 4 putative NAMs (compounds 3, 5, 6 and 36). In the paper enclosed with the thesis, we do not give names or show structures of these compounds to ensure the securing of intellectual property rights.

4.3. Paper 3

Freyd, T., Hendrickx, J., Sylte, I and Gabrielsen, M. (2018) **Opening of an intracellular water channel in the metabotropic glutamate receptor 1 by a positive allosteric modulator with intrinsic agonist properties.** *Manuscript*.

The x-ray crystal structure of $mGlu_1$-R in complex with the NAM FITM (PDB id 4OR2, (Wu et al., 2014)) was used as a starting point for MD simulations studying the interactions of allosteric modulators within the 7TM of the $mGlu_1$-R. We were using $mGlu_1$-R since the x-ray structure of the $GABA_{B2}$-R is not known. Non-biased MD simulations were run for 2μs for $mGlu_1$-R in complex with a FITM (NAM), VU0487351 (PAM) or VU0486321 (agoPAM).

FITM stabilized an inactive conformation very similar to its crystal structure but with a flip of the FITM in the binding pocket and the formation of a small α helix in the modelled part of ICL2. A part of this loop is not complete in the x-ray crystal structure and was modelled.

Both PAM and agoPAM moved in the binding pocket. The PAM moved slightly deeper into the intracellular side, while the agoPAM moved upwards very early in the simulation. By analysing the position of water molecules over time, we identified several hydration points (presence of water >90% of the time frames). The location of these hydration points was ligand specific and their position were similar to that of crystallographic water molecules found in $mGlu_5$-R experimental structures (Christopher et al., 2018). In a shallow binding pocket located in the vicinity the compounds formed by the extracellular ends of TM3-4-5 and ECL2, five hydrations points were identified for the $mGlu_1$-R:NAM, two for the $mGlu_1$-R:PAM, but none for the $mGlu_1$-R:agoPAM complex. The reason for that was that the upward movement of the agoPAM destroyed the hydrogen bonding network of the water molecules within this shallow pocket.

Two ionic locks have been identified in all experimental structures of $mGlu_1$-R and $mGlu_5$-R between TM3-TM6 and TM3-TM7. During the MD simulation with the $mGlu_1$-R:agoPAM the ionic locks were shifting partners and included amino acids in TM3, TM6, TM7 and ICL1. This shift was possible for two reasons: 1. -Unfolding of a small helix in ICL1, which is present in all available x-ray crystal structures of mGlu-Rs (Christopher et al., 2015, 2018; Doré et al., 2014; Wu et al., 2014). 2. -Anticlockwise rotation of the intracellular end of TM7 when seen from the bottom. Further, the rotation of the side chain of $F831^{7.53a.48c}$ allowed water molecules to penetrate higher into the receptor from the intracellular part creating a water channel. These changes and formation of the water channel were not observed during MD with the $mGlu_1$-R:NAM and $mGlu_1$-R:PAM complexes.

5. Discussion

GPCRs are interesting drug targets as they regulate important cellular processes and are involved in numerous diseases. Several family C GPCRs have been found to be putative drug targets in different neurological and neuropsychiatric disorders. The $GABA_B$-R has an inhibitory function in the CNS and is considered a drug target in several diseases including anxiety, depression, schizophrenia, pain, epilepsy, drug addiction, muscle spasticity and gastrointestinal reflux disorder (Brown et al., 2015; Cryan and Kaupmann, 2005; Lehmann et al., 2012). The mGlu-Rs are considered drug targets in disorders such as depression and anxiety, schizophrenia, epilepsy, Parkinson disease, and Fragile X syndrome (Alexander and Godwin, 2006; Gregory et al., 2013a; Masilamoni and Smith, 2018; Michalon et al., 2012; Moghaddam, 2004; Ngomba and van Luijtelaar, 2018; Niswender and Conn, 2010; Pilc et al., 2008; Sebastianutto and Cenci, 2018; Swanson et al., 2005)

The recent breakthroughs in GPCRs 3D structures with the release of at least one 3D structure from each of the main GPCR families have given incredible tools for SBDD. Structurally and functionally, the family C members are somewhat different as they contain a large extracellular VFT domain where orthosteric compounds bind. The first 3D structures of the 7TM domain from family C members, the $mGlu_1$-R (Wu et al., 2014) and $mGlu_5$-R (Doré et al., 2014), gave insight into their 3D structure and function. However, only crystal structure of GPCRs family C members in complex with NAMs, and none with PAMs are available so far, and hence SBDD strategies must take that into consideration when searching for new PAMs or in modelling studies with PAMs. These 3D structures also serve as a starting point for homology modelling of other family C GPCRs. We have used these structures, together with templates from family A and B, to generate $GABA_{B2}$-R models as described in paper 1.

The aim for constructing the models was to establish a ligand- and structure-based VS campaign for identifying new $GABA_B$-R modulators (paper 1&2). The known PAMs were used to screen an assembled database containing altogether 8.2 million compounds available for purchasing. This was done by deriving the physicochemical properties hold by known PAMs for $GABA_B$ and by generated pharmacophore models for each of the 5 structural clusters of known PAMs. The cured database was then docked into the 8 selected $GABA_{B2}$-R homology models from paper 1 to select putative new AMs for further experimental validation. The initial *in vitro* screening verification indicated that several

of the tested compounds are putative PAMs or NAMs, indicating that the established VS approach is functioning.

The increasing number of new compounds for the different family C receptors during the last years are aiding in SAR studies and provide tools to understand the pharmacology and molecular mechanism of action of these receptors. New family C compounds and structural information about the receptors facilitate experimental and theoretical studies of the mechanistic link between the allosteric and orthosteric binding pockets, and also about the signal biasing. In order to identify AM induced conformational changes upon binding, complexes of the x-ray structure of $mGlu_1$-R with NAM, PAM and agoPAM were studied by running 2 μs of non-biased MD simulations (paper 3).

5.1. Virtual screening in search for new $GABA_B$ allosteric modulators (paper 1 & 2)

5.1.1. Ligand-based approach (paper 2)

Ligand-based techniques are using structural information from active and inactive compounds to identify new compounds structurally resembling known active compounds. This strategy is best performing when a large set of compounds representing a broad structural diversity is available for the target. The search for known $GABA_B$-R compounds in the scientific literature resulted in 72 PAMs and a couple of NAMs. The PAMs were from patents and series of synthesised PAMs used for *in vitro* screening efforts. 72 PAMs must be considered as a quite limited number, hence limiting the chemical space we were working with. The PAMs were grouped into 5 structural clusters representing the chemical diversity of the known PAMs.

When the database of compounds for screening was assembled, several filtering steps were used in order to filter out the compounds, keeping only those fitting our aim. The first step, ADMET filtering also included physicochemical properties derived from known PAMs. As no pharmacophore models were able to match all PAMs, several pharmacophores models were generated based on the different clusters of known PAMs. The generated pharmacophores were then employed to reduce the database from 5 million to 8021 unique compounds. The majority of these compounds were from the output of the clusters 3 pharmacophore model (paper 2). Cluster 3 contained the largest number of known PAMs in original clustering of known PAMs and was also the structurally most diverse cluster. The diversity of the ligands in cluster 3 might explain why no cluster specific $GABA_{B2}$-R models were identified in paper 1.

5.1.2. Structure-based approach (paper 1)

The 3D structure of 7TM domain $GABA_{B2}$-R is unknown, and the homology modelling approach was selected for generating models due to the availability of templates from family A, B and C. The homology models were evaluated by docking of known $GABA_B$-R PAMs and decoys to identify cluster specific models. The use of known ligands to select and train the homology models was performed as it has already been used successfully by the Carlson group during the GPCR dock 2013 (Rodríguez et al., 2014) and other studies where ligands and experimental results were included as guidelines during the modelling (Carlsson et al., 2011; Cavasotto et al., 2008, 2008; Evers and Klebe, 2004; McRobb et al., 2010; Phatak et al., 2010). By using known ligand to guide the modelling, it permitted the incorporation of experimental data into the models, and hence increase the chances to model reliable conformations. This may also reduce the number of false positive but limits the conformational space of the AMs binding the models. However, the use of multiple conformations of the receptor in the screening may account for structural flexibility, which may help to identify more diverse ligands during the VS.

The first 600 homology models had poor BEDROC values, hence representing non-optimized conformations of the receptor which were not very prominent to rank the known PAMs in front of inactive compounds and decoys. The use of IFD improved the models as determined by the increased BEDROC scores (paper 1). Most probably, similar results could have been achieved by running MD simulations but it would have required more time and analysis. Not surprisingly the $GABA_{B2}$-R models based on mGlu-Rs seemed to be lot more accurate than models based on templates from family A and B. This was expected due to their higher sequence identity and functional similarities with $GABA_{B2}$-R compared to the other templates. Seven out of the eight selected cluster-specific models were generated from mGlu-R templates.

We mapped the putative allosteric binding pocket of $GABA_{B2}$-R to 24 residues, and we also proposed 9 residues as “hot spots” when considering all models. However, when considering only the models based on mGlu-R templates, we could increase these numbers to 25 and 13 residues, respectively (paper 1). The putative allosteric pocket of $GABA_B$-R was very hydrophobic. This was also reflected by the pharmacophore models for the clusters of the known PAMs, which hold multiple hydrophobic and at least one

aromatic feature (paper 2) and also by the 55 compounds selected for in vitro testing. Of those, 3 were put aside due to solubility issue.

The allosteric binding pockets of $mGlu_1$- and $mGlu_5$-R s and their co-crystalized ligands are also hydrophobic (Christopher et al., 2015, 2018; Doré et al., 2014; Wu et al., 2014). During the MD simulation of the $mGlu_1$-R:PAM complex, all direct protein-ligand interactions were hydrophobic (paper 3). These results fit well with the theory that AMs are rather hydrophobic compounds (Smith et al., 2017).

Despite having templates available, the modelling was challenging. The quite few PAMs available for $GABA_B$-R gives quite low structural diversity, and in addition, the sequence identify between the $GABA_{B2}$-R and the templates were only 10-20 %. Usually, it is recommended to have 30 % sequence identity to build reliable models of membrane proteins (Forrest et al., 2006). The difficulty of such modelling was well illustrated by the results of the last GPCR Dock 2013 with the modelling of the Class F smoothened (SMO) receptor. The closest template had 14 % sequence identify and the median 7TM RMSD of the models proposed was of 6.13 Å and 10.66 Å for the binding pockets (Kufareva et al., 2014). Even if the sequence identity between $GABA_{B2}$-R and the templates was higher, it would still be difficult to detect the smaller subpockets located within the binding pocket. For instance, a small subpocket is present in the allosteric pocket of $mGlu_5$-R and is proposed to play a role in ligand specificity (Doré et al., 2014; Harpsøe et al., 2017). This subpocket is not present in $mGlu_1$-R (Wu et al., 2014) and probably in none of the family C members (Harpsøe et al., 2015).

5.1.3. Target-based screening of the filtered database

Ligand binding is a dynamic process introducing conformational changes both into the ligand and the receptor (Vogt and Di Cera, 2013). Structure-based techniques use the knowledge about the structure of the target to predict the strength of the interaction with putative new compounds. It also helps to identify the necessary structural physiochemical properties that active or inactive compounds should hold to exert their activity. Atomic resolution structures from x-ray crystallography studies are recommended for the structure-based screening, but there are several reports successfully using high quality homology models for the structure-based approach (Carlsson et al., 2011; Gabrielsen et al., 2012; Ripphausen et al., 2010).

Traditionally, a structure-based VS is performed by using a rigid protein and flexible compounds. A rigid protein may be a limitation for the VS, as the conformation of the active site used in the screening is dependent on the structure of the co-crystallized ligand. This may induce a bias into the screening. In order to introduce flexibility, we have used multiple conformations of the $GABA_{B2}$-R in the screening process. The eight selected models from paper 1 were employed for the screening of the database, as each of them might represent information about the real binding pocket and together account for receptor flexibility. Due do the relatively low number of compounds to screen (8021), semi-flexible docking was employed and the top 10 % of the poses was kept for further scoring with MM-GBSA. The MM-GBSA method is very appropriate for ranking compounds as a certain correlation can be found between the calculated and the experimental binding energies (Du et al., 2011; Tripathi et al., 2015) but the calculated binding energies are not accurate compared with *in vitro* measurements, and should mainly be used for a relative ranking.

A selection of compounds for *in vitro* validation was done due to the limit of time, budget and capacity. Hence, we did not discriminate between the models and preselected the 20 ligands with the best MM-GBSA score from each model for further selection giving a total of 134 unique compounds. All 134 compounds were clustered and those that were identified among the best in more than one model were automatically selected. The selection of the compounds to purchase was done such that all clusters were represented among the preselected. The similarities with known PAMs were also taken into account. Compounds more dissimilar to known PAMs and with good scoring were preferred. The initial *in vitro* experiments identified novel NAMs and PAMs. This indicates that we have established a VS approach that functions and that homology modelling can be used to find AMs for $GABA_B$-R. The preliminary results are encouraging and more testing is necessary. If these compounds are not future drugs, they still are important research tools.

The use of MODELLER to generate several models from each template, and the technique of IFD may have limited putative template bias. In addition, among the hits both NAMs and PAMs were confirmed by *in vitro* testing (paper 2) despite using models trained with known PAMs only (paper 1). It means that we might have the correct binding pocket (or parts of it) and that PAM and NAMs have a very similar and overlapping binding pockets within the 7TM of $GABA_{B2}$-R. It has recently also been demonstrated that CLH304, a specific NAM for $GABA_B$-R, binds in the 7TM bundle of $GABA_{B2}$-R (Sun et al.,

2016). Our results are in accordance with the results of other family C members, indicating that PAM and NAM share a similar binding pocket (Harpsøe et al., 2017).

A question is if the structure-based approach was necessary to identify the AMs. Both the ligand-based and the structure-based approaches are known to give false positives. By using a combination of both methods, we intended to decrease the number of false positives and to bypass the limitations discussed above. In addition, it helped us to evaluate compounds from the ligand-based approach before purchasing.

5.1.4. Conclusion and further studies

We have established a VS protocol combining ligand- and structure-based techniques. To our knowledge, we are the first to provide an atomic-resolution description of the allosteric binding pocket of the $GABA_{B2}$-R in complex with PAMs. We are also the first to present new AMs for $GABA_B$-R using a VS campaign. The experimental testing confirmed the identification of both NAMs and PAMs for $GABA_B$-R. These results will help further studies on $GABA_B$-R, and help to increase the diversity of ligands available for the receptor which have huge potentials as drug target for brain disorders.

We have proposed potential residues important for binding of PAMs in the 7TM of $GABA_{B2}$-R. The features for NAMs have been grasped as we were able to identified both NAMs and PAMs, supporting that the binding pocket of NAMs and PAMs are overlapping.

In order to confirm that we have mapped the correct allosteric pocket of $GABA_B$-R in the homology models, *in vitro* experimental studies are needed. Site direct-mutagenesis studies of the suggested hot spot residues would be helpful for further evaluation of the homology models. However, the optimal would be an experimental structure of the 7TM domain of the $GABA_{B2}$-R.

The identified hits from the initial screening need to be further tested for complete characterisation of dose-response relationships and also to be tested for biased signalling. Additional cellular assays must be established to study potential biased signalling of the compounds. Postsynaptic $GABA_B$-R activation results in opening of G-protein-coupled inwardly-rectifying potassium (Kir/GIRK) channels, giving slow inhibitory post-synaptic potentials (Chalifoux and Carter, 2010). $GABA_B$-R activation also promotes the entry of calcium into the cell (Meier et al., 2008; New et al., 2006; Park et al., 2010). Finally, postsynaptic $GABA_B$-R activation also induces phosphorylation of extracellular signal-regulated protein kinases 1/2 (ERK1/2) in hippocampus and

cerebellum (Im and Rhim, 2012; Tu et al., 2007). Therefore, cellular assays for $GABA_B$-R mediated ERK1/2 phosphorylation, calcium mobilization and potassium efflux must be established to study the novel compounds.

5.2. Mechanisms of allosteric modulation (paper 3)

The mGlu-Rs are also interesting drug targets as they are involved in numerous diseases. The releases of the crystal structures of $mGlu_1$-R and $mGlu_5$-R in complex with NAMs was a breakthrough for SBDD for compounds targeting mGlu-Rs (Doré et al., 2014; Wu et al., 2014). Limited information is available about the structural features giving NAM, PAM and agoPAM activity. In the literature we identified a PAM and an agoPAM both specific for $mGlu_1$-R (Garcia-Barrantes et al., 2016). They were structurally very similar, and hence very interesting to study in order to understand the mechanism giving differences in their biological characteristics. The communication link between the allosteric binding site in the 7TM and the orthosteric pocket located in the extracellular VFT is still unknown. Only an inactive conformation of $mGlu_1$-R is available, hence we are lacking details about the dynamics of the receptor. A way to reach this goal is to employ MD simulations. A proposed model suggested that a mGlu-R needs 50 ms for complete activation from orthosteric binding to G-protein activation and that a 7TM might need 15 ms to turn to an active form (Rondard and Pin, 2015). Simulation of the millisecond time scale is not available commonly unless using dedicated hardware like the supercomputer Anton (Shaw et al., 2008). Thus, we knew in forehand that μs simulations would not be long enough to observe major larger movements connected to activation.

Using the inactive crystal structure of $mGlu_1$-R in complex the NAM FITM and in complex with the docked PAM (VU0487351) and agoPAM (VU0486321), we investigated the modulator induced conformational changes into the 7TMs upon binding by running 2μs of non-biased MD simulations. We intended to observe differences at the binding site between the AMs to understand the binding mechanism, and if the AMs could induce local differences into the allosteric $mGlu_1$-R protomer. We aimed to used $mGlu_1$-R as a model system for family C members. We consider our results as very interesting and they are in agreement with other published studies on mGlu-Rs.

As expected, the simulation of the $mGlu_1$-R:NAM complex was stable and no major changes into the receptor were observed. The amide moiety of the NAM FITM flipped but this was not novel as it has already seen by others (Harpsøe et al., 2015; Pérez-Benito et

al., 2017). Three overlapping binding pockets were identified. Between NAM and PAM pockets a slight difference was seen at the intracellular direction of the binding pocket. While the NAM, FITM, was interacting with TM6, the PAM, VU0487351, interacted at the interface of TM3-TM7. The overlapping of PAM and NAM pockets was in accordance with an extensive review of directed mutagenesis studies of family C members which concluded than PAM and NAM pockets are overlapping, but with some residues specific for both of them (Harpsøe et al., 2017). Based on studies of $mGlu_4$-R, the location of the binding site responsible for agoPAM activity have been suggested to be located at the top of the 7TM bundle corresponding to the orthosteric binding site found in family A members (Rovira et al., 2015). Our results are in accordance with that. In the very first ns of the simulation, the agoPAM moved upward with its furan moiety entering a shallow pocket located at the top of the receptor delimited by TM3-4-5. It corresponded to the pocket responsible for agoPAM activity in $mGlu_4$-R. In addition, the corresponding pocket is filled with crystal water molecules in the $mGlu_5$-R crystal structures. The most hydrated among them is the $mGlu_5$-R co-crystalized with the NAM MPEP (PDB code 6FFI, Christopher et al., 2018). Note that no water molecules were found in the entire experimental structure of $mGlu_1$-R (Wu et al., 2014).

Water molecules play very important roles in structural biology, in protein structures or to mediate protein-ligand interactions. By following the positions of the water molecules during the simulations, we described several hydration points, meaning that waters molecules are present at this peculiar position >90% of the MD frames considered.

Several of the identified hydration points could be superimposed with water molecules found in the experimental structure of $mGlu_5$-R in complex with the NAM MPEP (PDB code 6FFI, Christopher et al., 2018), which comforted us about the reliability of our results. The identified positions of the hydration points were rather specific for each of the AMs but with some resemblance. This was the case in the shallow pocket where the furan ring of the agoPAM was binding. During the simulation with $mGlu_1$-R:NAM, a stable water network was formed in the shallow pocket during the simulation. The position of the hydration point were matching the position of crystal water molecules s found in the x-ray crystal structure of $mGlu_5$-R :MPEP. During the simulation of $mGlu_1$-R:PAM, less stable water molecules were found in this subpocket, while non for the agoPAM. Hence the degree of solvation of the pocket might be dependent of the activity of the AMs or it could also be completely ligand-dependant.

Multiple of the hydration points were mediating protein-ligand interactions. For instance with the PAM, all the detected protein-ligand interaction were either direct hydrophobic bonds or water mediated polar interactions. A network of water molecules was linking PAM to N760$^{5.47ac}$, Y672$^{3.40a.44c}$ and S822$^{7.45a.39a}$. N760$^{5.47ac}$ and Y672$^{3.40a.44c}$ are suggested to be part of a "trigger switch" and "transmission switch" respectively (Pérez-Benito et al., 2017). Similarly, a water-network was linking agoPAM to N760$^{5.47ac}$ and S822$^{7.45a.39a}$. NAM was also interacting with N760$^{5.47ac}$ but no direct or indirect interaction with the "transmission switch" was observed. In all simulations, a hydration point was found deep in the binding pocket and coordinated by the residues Y672$^{3.40a.44c}$, T794$^{6.44a.46c}$ and S822$^{7.45a.39c}$. This hydration point corresponds to a crystal water molecule found in all experimental structures of $mGlu_5$-R (Christopher et al., 2015, 2018; Doré et al., 2014). Studies indicate that perturbation of the network in this region could be responsible for the pharmacological mode-switching seen with several series of $mGlu_5$-R AMs (Christopher et al., 2018; Doré et al., 2014; Harpsøe et al., 2015).

An ionic lock has been described in 50 % of family A members and demonstrated to stabilize the receptor in an inactive position by holding TM6 in place. If not present, another set of interactions fulfil the same function. The breakage of this lock is a prerequisite for a fully activation of family A members. A similar ionic lock has been described for family C members, and its importance was revealed by a study on $GABA_B$-R (Binet et al., 2007). This ionic lock is present in the crystal structure of $mGlu_1$- and $mGlu_5$-R (Doré et al., 2014; Wu et al., 2014). In $mGlu_1$-R it links E783$^{6.33a.35c}$ with K834$^{7.51a.57c}$ with stabilizing polar interaction with serines in ICL1 and strengthens the lock. In an MD study of $mGlu_4$-R in complex with the PAM MPEP (Dalton et al., 2017), the ionic lock was seen to be less stable which were not observed in our case. They also simulated the $mGlu_5$-R :MPEP complex, and in that receptor this ionic interaction was stable throughout the MD, which is in line with our results where the ionic interaction between E783 and K834 was stable for the MD simulation of NAM, PAM and agoPAM.

5.2.1. Activations features

Yuan et al. (Yuan et al., 2014) managed to identify layers of hydrophobic residues in family A GPCRs that impair the movements of water molecules within the receptors. One of these layers is including Y7.53a in the NPxxY motif found in TM7 of family A GPCRs. Tehan et al. (Tehan et al., 2014) also predicted a similar mechanism, and that during the activation of family A GPCRs, there is rearrangement of hydrophobic residues which

allow the creation of a water channel close to the NPxxY motif. They called it the hydrophobic hindering mechanism (HHM). Yuan at al. notably demonstrated that the creation of a water channel was dependant of the conformations of $Y^{7.53a}$. In $mGlu_1$-R and in $mGlu_5$-R, the residue corresponding to $Y^{7.53a}$ is $F^{7.53a.48c}$. The neighbouring residue is $M^{7.47c}$. Crystal water molecules are located below these two residues in the x-ray crystal structures of $mGlu_5$-Rs. In $mGlu_1$-R, these two positions correspond to $M830^{7.47c}$ and $F831^{7.53a.48c}$. In the simulations with NAM and PAM, both residues maintained stable conformations similar to that in the crystal structure. On the other hand, at the end of the $mGlu_1$-R:agoPAM simulation, TM7 did a clockwise rotation when seen from the top of the receptor, bringing the side chain of $F831^{7.53a.48c}$ outside of the bundle and the side chain of $M830^{7.47c}$ to a position corresponding to the previous location of $F831^{7.53a.48c}$ before the rotation. This helical rotation created a space which was filled with water molecules that were entering and could formed contact with the layer of water molecules at the bottom of the allosteric pocket (see above), creating a water channel from the intracellular end up to the allosteric binding pocket. This rotating mechanism that generates a water channel from the intracellular side of the receptor may apply to all mGlu-R and $GABA_B$-R, as the bulky character is conserved in position 7.53a.48c as well as the hydrophobic profile in position 7.47c (Pándy-Szekeres et al., 2018).

One the major movements during activation of family A members is the outward movement of TM6 to unveil the G-protein coupling site. Xue et al. (Xue et al., 2015) demonstrated with their work on $mGlu_2$-R that upon activation, the interface of contacts between the protomers of $mGlu_2$-R changed from TM4-5 to TM6. The shallow pocket that the furan moiety of agoPAM was occupying during the simulation was partly created by TM4 and TM5. Dalton et al. also mentioned that TM6 was rigid during the MD simulation of $mGlu_4$-R:MPEP, and hence TM6 might not have the same role as seen in family A (Dalton et al., 2017). Our results indicate the same, and this is also is realistic since the other protomer may be connected by TM6 contacts (Xue et al., 2015). Due to the dimer interface interactions, TM6 might have difficulty to perform an outward movement when activated. Though, TM7 could be actually the helix than play a pivot role in mGlu-Rs activation (see previous paragraph).

Evidences for potential activation features were also observed in ICLs of the 7TM bundle of $mGlu_1$-R. Within the modelled part of ICL2, a stable small α-helix was formed during the last 500 ns of the simulation of $mGlu_1$-R:NAM, but some conformations with

such an helix was seen around 1 μs of the simulation of $mGlu_1$-R:PAM, while ICL2 in the $mGlu_1$-R:agoPAM simulation stayed unordered during the entire simulation. The opposite was seen for the β2-AR; ICL2 was unfolded in the inactive form (PDB code 2RH1, Cherezov et al., 2007), while a small α-helix is present in the active conformation and found to interact with the G-protein (PDB code 3SN6, Rasmussen et al., 2011). In every experimental structures of mGlu-Rs (except for $mGlu_1$-R which is unordered in this region) an α-helix is present in ICL1, and we identified the same in our $mGlu_1$-R:NAM simulation. Using $mGlu_4$-R in complex with the PAM MPEP, Dalton et al observed a partial unfolding of ICL1 during a 5μs MD. We did not observed the same in our simulation of $mGlu_1$-R:PAM, but it was observed around 1 μs for the simulation of $mGlu_1$-R:agoPAM as the distance $E783^{6.33a.35c}$-$S626^{ICL1}$ increased. The unfolding of ICL1 reoriented $K624^{ICL1}$ which caused instability in the ionic lock ($E783^{6.33a.35c}$-$K834^{7.51a.57c}$).

An second ionic lock can also be found in all x-ray crystal structure of mGlu-Rs between TM3 and TM7 (Christopher et al., 2015, 2018; Doré et al., 2014; Wu et al., 2014). This corresponds to the ionic interaction $E783^{6.33a.35c}$-$K834^{7.51a.57c}$ in $mGlu_1$-R. During the simulation of $mGlu_1$-R with NAM and PAM, this interaction is stable. For the agoPAM simulation, the distance between these two residues increased at about 1.85 μs. On the other hand, the distance between $E783^{6.33a.35c}$ and $K624^{ICL1}$ decreased. As mentioned before there is a rotation of the intracellular part of TM7 at the end of the agoPAM simulation, apart its effects on $F831^{7.51a.57c}$, this rotation also moved the side chain of $K834^{7.51a.57c}$ away, and hence $K624^{ICL1}$ took its place to form a new ionic lock. This exchange could be plausible in all mGlu-R as this lysine in TM7 is conserved, and it is also conserved in both subunits of the $GABA_B$-R. The lysine in ICL1 is also present in all these family C receptors, but in the $GABA_{B1}$-R subunit where it is a glutamine. This is interesting since the $GABA_{B1}$-subunit is not able to couple with G-proteins.

Chloride is known to be a PAM for $mGlu_1$-R and has been demonstrated to exert its activity at the VFT domain (Tora et al., 2015). Nevertheless, we have observed a chloride ion mainly coordinated by $R681^{3.49a.53c}$ and $K678^{3.46a.50c}$ during the simulations with NAM and PAM. In mGlu1:agoPAM simulation, after the exchange of ionic partners (see above), $K624^{ICL1}$ also coordinated the chloride together with $R681^{3.49a.53c}$ and $K678^{3.46a.50c}$. Serine residues from ICL1 and water molecules were also coordinating the chloride during periods of the simulations. It might be an artefact and more studies are needed to confirm that a chloride-binding site exists. Nevertheless, similar results have been seen in MD

simulation of our $GABA_{B2}$ models generated in paper 1 (unpublished work) and within the x-ray crystal structure of $mGlu_5$-R both in complex with the NAM mavoglurant (PDB id 4oo9, Doré et al., 2014) and in the apo form (unpublished work).

Finally, we arrived at the same conclusion for our simulation with agoPAM as that of Dalton et al. for their $mGlu_4$:MPEP simulation that the receptor achieved a more open intracellular conformation with longer distance between the ICLs and a more hydrated receptor. A water channel opening up from the intracellular part was observed during the agoPAM simulation. The existence of such water channel has already been proposed for GPCR family A (Tehan et al., 2014; Yuan et al., 2014).

5.2.2. Conclusion and perspective

Through non-biased MD simulations, we have analysed the induced conformational changes upon binding of different AMs for $mGlu_1$-R. We have identified the agoPAM binding pocket in $mGlu_1$-R and shown that it is overlapping with the pockets of NAM and PAM. We have also seen that agoPAM induced conformational changes generating differences in the network of water molecules compared the PAM and NAM, that may be connected to receptor activation. The changes were triggered by numerous conformational changes that may be extrapolate to others family C GPCRs. These conformational changes were not seen for the other AMs.

In order to confirm our findings, *in vitro* site directed mutagenesis studies could be performed, but also *in silico* approaches could be used to further study these processes. Reproducing the same results should be achievable by running the same protomer with another agoPAM or with a $mGlu_5$-R:agoPAM complex or at best by running the simulation of both $mGlu_1$-R and $mGlu_5$-R.

Also, the dynamic of the $GABA_B$-R should be study by tempting to run MD simulation in the same condition as we did in this thesis to confirm the conservation of the features of activation we have detected in $mGlu_1$-R-agoPAM within family C members.

6. Conclusion

GPCRs are major drug targets being involved in the biological functions of the human body and in the pathophysiology of diseases. Despite several decades of GPCR research, there is still a lot unknown about the structure and function of GPCRs, and their roles in disease mechanism and as therapeutic targets. $GABA_B$-R and mGlu-Rs are targets for the treatments of several CNS disorders. The potential advantages of allosteric compounds hold strong hopes for the design of more selective drugs.

In the present study, we have built multiple homology models of the TM-part of $GABA_{B2}$-R that might represent putative conformations of the allosteric binding pocket as they could accommodate the known PAMs (paper 1). Several residues of the binding pockets were identified as the potential determinants for PAM binding and specificity to $GABA_{B2}$-R.

Both ligand and target structure information were merged in a hybrid VS approach. The homology models were used for screening of a filtered database and for guiding selection of compounds for *in vitro* testing. This strategy was successful as several novel NAMs and PAMs were identified. To our knowledge, this is the first study identifying $GABA_B$-R AMs using an *in silico* VS strategy (paper 2). In line with other studies on other family C receptors and $GABA_B$-R, these results shown that NAMs and PAMs might share an overlapping binding pocket in the 7TM bundle of the $GABA_{B2}$-R.

MD simulation techniques are helpful for a better understanding of the dynamic of a receptor and the structural effects upon ligand binding. Hence, the structural differences observed during the simulations of the 7TM domain of $mGlu_1$-R in complex with a NAM, PAM and agoPAM would be valuable information for further work on family C members or to help designing *in vitro* experiments.

Water molecules might play a crucial role in ligand binding and activation of GPCRs (Christopher et al., 2018; Yuan et al., 2014). During MD simulations we identified ligand specific hydration points within the binding pocket of $mGlu_1$-R that may be connected to activation and the differences between NAM, PAM and agoPAM activity. Our studies also indicated the importance of water molecules for binding and activity, and that water molecules should be taken into account in drug design. The identification of a water channel within the 7TM domain of $mGlu_1$-R as observed at similar regions in family A may suggest that this is a common feature among GPCRs of family A and C.

GPCRs are, and still hot targets in drug discovery. The knowledge about these receptors will increase with the improvement of technology. Very recently (between the 13th and the 20th of June, 2018) four experimental structures of family A GPCRs in complex with G-proteins were released. These structures were resolved with the technique of cryo-electron microscopy, which is a technique with huge improvements during the last years, also resulting in the Nobel Prize in Chemistry for 2017 (https://www.nobelprize.org/nobel_prizes/chemistry/laureates/2017/press.html).
There are still a lot to discovery about GPCRs, and hopefully the results in the present thesis are a support for further GPCR research.

7. References

Alexander, G.M., and Godwin, D.W. (2006). Metabotropic glutamate receptors as a strategic target for the treatment of epilepsy. Epilepsy Res. *71*, 1–22.

Banks, J.L., Beard, H.S., Cao, Y., Cho, A.E., Damm, W., Farid, R., Felts, A.K., Halgren, T.A., Mainz, D.T., Maple, J.R., et al. (2005). Integrated Modeling Program, Applied Chemical Theory (IMPACT). J. Comput. Chem. *26*, 1752–1780.

Berry-Kravis, E., Hessl, D., Coffey, S., Hervey, C., Schneider, A., Yuhas, J., Hutchison, J., Snape, M., Tranfaglia, M., Nguyen, D.V., et al. (2009). A pilot open label, single dose trial of fenobam in adults with fragile X syndrome. J. Med. Genet. *46*, 266–271.

Berry-Kravis, E., Des Portes, V., Hagerman, R., Jacquemont, S., Charles, P., Visootsak, J., Brinkman, M., Rerat, K., Koumaras, B., Zhu, L., et al. (2016). Mavoglurant in fragile X syndrome: Results of two randomized, double-blind, placebo-controlled trials. Sci. Transl. Med. *8*, 321ra5.

Binet, V., Brajon, C., Corre, L.L., Acher, F., Pin, J.-P., and Prézeau, L. (2004). The Heptahelical Domain of GABAB2 Is Activated Directly by CGP7930, a Positive Allosteric Modulator of the GABAB Receptor. J. Biol. Chem. *279*, 29085–29091.

Binet, V., Duthey, B., Lecaillon, J., Vol, C., Quoyer, J., Labesse, G., Pin, J.-P., and Prézeau, L. (2007). Common Structural Requirements for Heptahelical Domain Function in Class A and Class C G Protein-coupled Receptors. J. Biol. Chem. *282*, 12154–12163.

Bordner, A.J. (2012). Force fields for homology modeling. Methods Mol. Biol. Clifton NJ *857*, 83–106.

Bowery, N.G. (1993). GABAB Receptor Pharmacology. Annu. Rev. Pharmacol. Toxicol. *33*, 109–147.

Bradley, S.R., Levey, A.I., Hersch, S.M., and Conn, P.J. (1996). Immunocytochemical localization of group III metabotropic glutamate receptors in the hippocampus with subtype-specific antibodies. J. Neurosci. Off. J. Soc. Neurosci. *16*, 2044–2056.

Brown, K.M., Roy, K.K., Hockerman, G.H., Doerksen, R.J., and Colby, D.A. (2015). Activation of the γ-Aminobutyric Acid Type B (GABA(B)) Receptor by Agonists and Positive Allosteric Modulators. J. Med. Chem. *58*, 6336–6347.

Calver, A.R., Robbins, M.J., Cosio, C., Rice, S.Q.J., Babbs, A.J., Hirst, W.D., Boyfield, I., Wood, M.D., Russell, R.B., Price, G.W., et al. (2001). The C-Terminal Domains of the GABAB Receptor Subunits Mediate Intracellular Trafficking But Are Not Required for Receptor Signaling. J. Neurosci. *21*, 1203–1210.

Carlsson, J., and Persson, B. (2011). Investigating Protein Variants Using Structural Calculation Techniques. In Homology Modeling, (Humana Press), pp. 313–330.

Carlsson, J., Coleman, R.G., Setola, V., Irwin, J.J., Fan, H., Schlessinger, A., Sali, A., Roth, B.L., and Shoichet, B.K. (2011). Ligand discovery from a dopamine D3 receptor homology model and crystal structure. Nat. Chem. Biol. *7*, 769–778.

Cavasotto, C.N., Orry, A.J.W., Murgolo, N.J., Czarniecki, M.F., Kocsi, S.A., Hawes, B.E., O'Neill, K.A., Hine, H., Burton, M.S., Voigt, J.H., et al. (2008). Discovery of Novel Chemotypes to a G-Protein-Coupled Receptor through Ligand-Steered Homology Modeling and Structure-Based Virtual Screening. J. Med. Chem. *51*, 581–588.

Cereto-Massagué, A., Ojeda, M.J., Valls, C., Mulero, M., Garcia-Vallvé, S., and Pujadas, G. (2015). Molecular fingerprint similarity search in virtual screening. Methods San Diego Calif *71*, 58–63.

Chalifoux, J.R., and Carter, A.G. (2010). GABAB receptors modulate NMDA receptor calcium signals in dendritic spines. Neuron *66*, 101–113.

Cherezov, V., Rosenbaum, D.M., Hanson, M.A., Rasmussen, S.G.F., Thian, F.S., Kobilka, T.S., Choi, H.-J., Kuhn, P., Weis, W.I., Kobilka, B.K., et al. (2007). High-resolution crystal structure of an engineered human beta2-adrenergic G protein-coupled receptor. Science *318*, 1258–1265.

Chothia, C., and Lesk, A.M. (1986). The relation between the divergence of sequence and structure in proteins. EMBO J. *5*, 823–826.

Christopher, J.A., Aves, S.J., Bennett, K.A., Doré, A.S., Errey, J.C., Jazayeri, A., Marshall, F.H., Okrasa, K., Serrano-Vega, M.J., Tehan, B.G., et al. (2015). Fragment and Structure-Based Drug Discovery for a Class C GPCR: Discovery of the mGlu5 Negative Allosteric Modulator HTL14242 (3-Chloro-5-[6-(5-fluoropyridin-2-yl)pyrimidin-4-yl]benzonitrile). J. Med. Chem. *58*, 6653–6664.

Christopher, J.A., Orgován, Z., Congreve, M., Doré, A.S., Errey, J.C., Marshall, F.H., Mason, J.S., Okrasa, K., Rucktooa, P., Serrano-Vega, M.J., et al. (2018). Structure-Based Optimization Strategies for G Protein-Coupled Receptor (GPCR) Allosteric Modulators: A Case Study from Analyses of New Metabotropic Glutamate Receptor 5 (mGlu5) X-ray Structures. J. Med. Chem.

Chung, K.Y., Rasmussen, S.G.F., Liu, T., Li, S., DeVree, B.T., Chae, P.S., Calinski, D., Kobilka, B.K., Woods, V.L., and Sunahara, R.K. (2011). β2 adrenergic receptor-induced conformational changes in the heterotrimeric G protein Gs. Nature *477*, 611–615.

Civelli, O., Reinscheid, R.K., Zhang, Y., Wang, Z., Fredriksson, R., and Schiöth, H.B. (2013). G Protein–Coupled Receptor Deorphanizations. Annu. Rev. Pharmacol. Toxicol. *53*, 127–146.

Conn, P.J., Christopoulos, A., and Lindsley, C.W. (2009). Allosteric modulators of GPCRs: a novel approach for the treatment of CNS disorders. Nat. Rev. Drug Discov. *8*, 41–54.

Conn, P.J., Lindsley, C.W., Meiler, J., and Niswender, C.M. (2014). Opportunities and challenges in the discovery of allosteric modulators of GPCRs for treating CNS disorders. Nat. Rev. Drug Discov. *13*, 692–708.

Costa, T., and Cotecchia, S. (2005). Historical review: Negative efficacy and the constitutive activity of G-protein-coupled receptors. Trends Pharmacol. Sci. *26*, 618–624.

Costanzi, S., Siegel, J., Tikhonova, I.G., and Jacobson, K.A. (2009). Rhodopsin and the others: a historical perspective on structural studies of G protein-coupled receptors. Curr. Pharm. Des. *15*, 3994–4002.

Cross, J.B. (2018). Methods for Virtual Screening of GPCR Targets: Approaches and Challenges. In Computational Methods for GPCR Drug Discovery, (Humana Press, New York, NY), pp. 233–264.

Cryan, J.F., and Kaupmann, K. (2005). Don't worry 'B' happy!: a role for GABAB receptors in anxiety and depression. Trends Pharmacol. Sci. *26*, 36–43.

Cvicek, V., Goddard, W.A., and Abrol, R. (2016). Structure-Based Sequence Alignment of the Transmembrane Domains of All Human GPCRs: Phylogenetic, Structural and Functional Implications. PLoS Comput. Biol. *12*.

D T Monaghan, R J Bridges, and Cotman, and C.W. (1989). The Excitatory Amino Acid Receptors: Their Classes, Pharmacology, and Distinct Properties in the Function of the Central Nervous System. Annu. Rev. Pharmacol. Toxicol. *29*, 365–402.

Dalton, J.A.R., Pin, J.-P., and Giraldo, J. (2017). Analysis of positive and negative allosteric modulation in metabotropic glutamate receptors 4 and 5 with a dual ligand. Sci. Rep. *7*, 4944.

Dickson, M., and Gagnon, J.P. (2004). Key factors in the rising cost of new drug discovery and development. Nat. Rev. Drug Discov. *3*, 417–429.

Doré, A.S., Okrasa, K., Patel, J.C., Serrano-Vega, M., Bennett, K., Cooke, R.M., Errey, J.C., Jazayeri, A., Khan, S., Tehan, B., et al. (2014). Structure of class C GPCR metabotropic glutamate receptor 5 transmembrane domain. Nature *511*, 557–562.

Dorr, P., Westby, M., Dobbs, S., Griffin, P., Irvine, B., Macartney, M., Mori, J., Rickett, G., Smith-Burchnell, C., Napier, C., et al. (2005). Maraviroc (UK-427,857), a potent, orally bioavailable, and selective small-molecule inhibitor of chemokine receptor CCR5 with broad-spectrum anti-human immunodeficiency virus type 1 activity. Antimicrob. Agents Chemother. *49*, 4721–4732.

Doumazane, E., Scholler, P., Zwier, J.M., Trinquet, E., Rondard, P., and Pin, J.-P. (2010). A new approach to analyze cell surface protein complexes reveals specific heterodimeric metabotropic glutamate receptors. FASEB J. *25*, 66–77.

Draper-Joyce, C.J., Khoshouei, M., Thal, D.M., Liang, Y.-L., Nguyen, A.T.N., Furness, S.G.B., Venugopal, H., Baltos, J.-A., Plitzko, J.M., Danev, R., et al. (2018). Structure of the adenosine-bound human adenosine A 1 receptor–G i complex. Nature.

Dror, R.O., Arlow, D.H., Maragakis, P., Mildorf, T.J., Pan, A.C., Xu, H., Borhani, D.W., and Shaw, D.E. (2011). Activation mechanism of the β2-adrenergic receptor. Proc. Natl. Acad. Sci. U. S. A. *108*, 18684–18689.

Du, J., Sun, H., Xi, L., Li, J., Yang, Y., Liu, H., and Yao, X. (2011). Molecular modeling study of checkpoint kinase 1 inhibitors by multiple docking strategies and prime/MM–GBSA calculation. J. Comput. Chem. *32*, 2800–2809.

Duan, J., Dixon, S.L., Lowrie, J.F., and Sherman, W. (2010). Analysis and comparison of 2D fingerprints: insights into database screening performance using eight fingerprint methods. J. Mol. Graph. Model. *29*, 157–170.

Dupuis, D.S., Relkovic, D., Lhuillier, L., Mosbacher, J., and Kaupmann, K. (2006). Point Mutations in the Transmembrane Region of GABAB2 Facilitate Activation by the Positive Modulator N,N′-Dicyclopentyl-2-methylsulfanyl-5-nitro-pyrimidine-4,6-diamine (GS39783) in the Absence of the GABAB1 Subunit. Mol. Pharmacol. *70*, 2027–2036.

Evers, A., and Klebe, G. (2004). Successful Virtual Screening for a Submicromolar Antagonist of the Neurokinin-1 Receptor Based on a Ligand-Supported Homology Model. J. Med. Chem. *47*, 5381–5392.

Fiser, A., and Šali, A. (2003). Modeller: Generation and Refinement of Homology-Based Protein Structure Models. In Methods in Enzymology, J. and R.M.S. Charles W. Carter, ed. (Academic Press), pp. 461–491.

Forrest, L.R., Tang, C.L., and Honig, B. (2006). On the Accuracy of Homology Modeling and Sequence Alignment Methods Applied to Membrane Proteins. Biophys. J. *91*, 508–517.

Frankowska, M., Filip, M., and Przegaliński, E. (2007). Effects of GABAB receptor ligands in animal tests of depression and anxiety. Pharmacol. Rep. PR *59*, 645–655.

Fredriksson, R., Lagerström, M.C., Lundin, L.-G., and Schiöth, H.B. (2003). The G-Protein-Coupled Receptors in the Human Genome Form Five Main Families. Phylogenetic Analysis, Paralogon Groups, and Fingerprints. Mol. Pharmacol. *63*, 1256–1272.

Friesner, R.A., Banks, J.L., Murphy, R.B., Halgren, T.A., Klicic, J.J., Mainz, D.T., Repasky, M.P., Knoll, E.H., Shelley, M., Perry, J.K., et al. (2004). Glide: a new approach for rapid, accurate docking and scoring. 1. Method and assessment of docking accuracy. J. Med. Chem. *47*, 1739–1749.

Gabrielsen, M., Kurczab, R., Ravna, A.W., Kufareva, I., Abagyan, R., Chilmonczyk, Z., Bojarski, A.J., and Sylte, I. (2012). Molecular mechanism of serotonin transporter inhibition elucidated by a new flexible docking protocol. Eur. J. Med. Chem. *47*, 24–37.

Gacasan, S.B., Baker, D.L., and Parrill, A.L. (2017). G protein-coupled receptors: the evolution of structural insight. Biophys. 2017 Vol 4 Pages 491-527.

Galvez, T., Urwyler, S., Prézeau, L., Mosbacher, J., Joly, C., Malitschek, B., Heid, J., Brabet, I., Froestl, W., Bettler, B., et al. (2000). Ca2+ Requirement for High-Affinity γ-Aminobutyric Acid (GABA) Binding at GABAB Receptors: Involvement of Serine 269 of the GABABR1 Subunit. Mol. Pharmacol. *57*, 419–426.

Galvez, T., Duthey, B., Kniazeff, J., Blahos, J., Rovelli, G., Bettler, B., Prézeau, L., and Pin, J.-P. (2001). Allosteric interactions between GB1 and GB2 subunits are required for optimal GABAB receptor function. EMBO J. *20*, 2152–2159.

Garcia-Barrantes, P.M., Cho, H.P., Blobaum, A.L., Niswender, C.M., Conn, P.J., and Lindsley, C.W. (2016). Lead optimization of the VU0486321 series of mGlu1 PAMs. Part

3. Engineering plasma stability by discovery and optimization of isoindolinone analogs. Bioorg. Med. Chem. Lett. *26*, 1869–1872.

García-Nafría, J., Nehmé, R., Edwards, P.C., and Tate, C.G. (2018). Cryo-EM structure of the serotonin 5-HT 1B receptor coupled to heterotrimeric G o. Nature 1.

Gassmann, M., and Bettler, B. (2012). Regulation of neuronal GABAB receptor functions by subunit composition. Nat. Rev. Neurosci. *13*, 380–394.

Geng, Y., Xiong, D., Mosyak, L., Malito, D.L., Kniazeff, J., Chen, Y., Burmakina, S., Quick, M., Bush, M., Javitch, J.A., et al. (2012). Structure and functional interaction of the extracellular domain of human GABAB receptor GBR2. Nat. Neurosci. *15*, 970–978.

Geng, Y., Bush, M., Mosyak, L., Wang, F., and Fan, Q.R. (2013). Structural mechanism of ligand activation in human GABAB receptor. Nature *504*, 254–259.

Ghose, S., Winter, M.K., McCarson, K.E., Tamminga, C.A., and Enna, S.J. (2011). The GABAB receptor as a target for antidepressant drug action. Br. J. Pharmacol. *162*, 1–17.

Gloriam, D.E., Fredriksson, R., and Schiöth, H.B. (2007). The G protein-coupled receptor subset of the rat genome. BMC Genomics *8*, 338.

Goudet, C., Gaven, F., Kniazeff, J., Vol, C., Liu, J., Cohen-Gonsaud, M., Acher, F., Prézeau, L., and Pin, J.P. (2004). Heptahelical domain of metabotropic glutamate receptor 5 behaves like rhodopsin-like receptors. Proc. Natl. Acad. Sci. *101*, 378–383.

Goudet, C., Rovira, X., Rondard, P., Pin, J.-P., Llebaria, A., and Acher, F. (2018). Modulation of Metabotropic Glutamate Receptors by Orthosteric, Allosteric, and Light-Operated Ligands. (Berlin, Heidelberg: Springer Berlin Heidelberg), p.

Gräter, F., and Li, W. (2015). Transition Path Sampling with Quantum/Classical Mechanics for Reaction Rates. In Molecular Modeling of Proteins, (Humana Press, New York, NY), pp. 27–45.

Gregory, K.J., Noetzel, M.J., and Niswender, C.M. (2013a). Pharmacology of metabotropic glutamate receptor allosteric modulators: structural basis and therapeutic potential for CNS disorders. Prog. Mol. Biol. Transl. Sci. *115*, 61–121.

Gregory, K.J., Nguyen, E.D., Reiff, S.D., Squire, E.F., Stauffer, S.R., Lindsley, C.W., Meiler, J., and Conn, P.J. (2013b). Probing the Metabotropic Glutamate Receptor 5 (mGlu5) Positive Allosteric Modulator (PAM) Binding Pocket: Discovery of Point Mutations That Engender a "Molecular Switch" in PAM Pharmacology. Mol. Pharmacol. *83*, 991–1006.

Harder, E., Damm, W., Maple, J., Wu, C., Reboul, M., Xiang, J.Y., Wang, L., Lupyan, D., Dahlgren, M.K., Knight, J.L., et al. (2016). OPLS3: A Force Field Providing Broad Coverage of Drug-like Small Molecules and Proteins. J. Chem. Theory Comput. *12*, 281–296.

Harpsøe, K., Isberg, V., Tehan, B.G., Weiss, D., Arsova, A., Marshall, F.H., Bräuner-Osborne, H., and Gloriam, D.E. (2015). Selective Negative Allosteric Modulation Of Metabotropic Glutamate Receptors – A Structural Perspective of Ligands and Mutants. Sci. Rep. *5*, 13869.

Harpsøe, K., Boesgaard, M.W., Munk, C., Bräuner-Osborne, H., and Gloriam, D.E. (2017). Structural insight to mutation effects uncover a common allosteric site in class C GPCRs. Bioinformatics *33*, 1116–1120.

Hauser, A.S., Attwood, M.M., Rask-Andersen, M., Schiöth, H.B., and Gloriam, D.E. (2017). Trends in GPCR drug discovery: new agents, targets and indications. Nat. Rev. Drug Discov. *16*, 829–842.

Hawkins, P.C.D., and Stahl, G. (2018). Ligand-Based Methods in GPCR Computer-Aided Drug Design. In Computational Methods for GPCR Drug Discovery, (Humana Press, New York, NY), pp. 365–374.

Herculano-Houzel, S. (2009). The Human Brain in Numbers: A Linearly Scaled-up Primate Brain. Front. Hum. Neurosci. *3*.

Hilger, D., Masureel, M., and Kobilka, B.K. (2018). Structure and dynamics of GPCR signaling complexes. Nat. Struct. Mol. Biol. *25*, 4–12.

Hollmann, M., and Heinemann, S. (1994). Cloned Glutamate Receptors. Annu. Rev. Neurosci. *17*, 31–108.

Horvath, D. (2010). Pharmacophore-Based Virtual Screening. In Chemoinformatics and Computational Chemical Biology, (Humana Press, Totowa, NJ), pp. 261–298.

Im, B.-H., and Rhim, H. (2012). GABA(B) receptor-mediated ERK1/2 phosphorylation via a direct interaction with Ca(V)1.3 channels. Neurosci. Lett. *513*, 89–94.

Kang, Y., Zhou, X.E., Gao, X., He, Y., Liu, W., Ishchenko, A., Barty, A., White, T.A., Yefanov, O., Han, G.W., et al. (2015). Crystal structure of rhodopsin bound to arrestin by femtosecond X-ray laser. Nature *523*, 561–567.

Kang, Y., Kuybeda, O., Waal, P.W. de, Mukherjee, S., Eps, N.V., Dutka, P., Zhou, X.E., Bartesaghi, A., Erramilli, S., Morizumi, T., et al. (2018). Cryo-EM structure of human rhodopsin bound to an inhibitory G protein. Nature 1.

Kaserer, T., Beck, K.R., Akram, M., Odermatt, A., and Schuster, D. (2015). Pharmacophore Models and Pharmacophore-Based Virtual Screening: Concepts and Applications Exemplified on Hydroxysteroid Dehydrogenases. Molecules *20*, 22799–22832.

Katritch, V., Fenalti, G., Abola, E.E., Roth, B.L., Cherezov, V., and Stevens, R.C. (2014). Allosteric sodium in class A GPCR signaling. Trends Biochem. Sci. *39*, 233–244.

Kelder, J., Grootenhuis, P.D.J., Bayada, D.M., Delbressine, L.P.C., and Ploemen, J.-P. (1999). Polar Molecular Surface as a Dominating Determinant for Oral Absorption and Brain Penetration of Drugs. Pharm. Res. *16*, 1514–1519.

Kniazeff, J., Galvez, T., Labesse, G., and Pin, J.-P. (2002). No Ligand Binding in the GB2 Subunit of the GABABReceptor Is Required for Activation and Allosteric Interaction between the Subunits. J. Neurosci. *22*, 7352–7361.

Kniazeff, J., Bessis, A.-S., Maurel, D., Ansanay, H., Prézeau, L., and Pin, J.-P. (2004). Closed state of both binding domains of homodimeric mGlu receptors is required for full activity. Nat. Struct. Mol. Biol. *11*, 706–713.

Koehl, A., Hu, H., Maeda, S., Zhang, Y., Qu, Q., Paggi, J.M., Latorraca, N.R., Hilger, D., Dawson, R., Matile, H., et al. (2018). Structure of the μ-opioid receptor–G i protein complex. Nature 1.

Kohl, M.M., and Paulsen, O. (2010). The roles of GABAB receptors in cortical network activity. Adv. Pharmacol. San Diego Calif *58*, 205–229.

Koulen, P., and Brandstätter, J.H. (2002). Pre- and Postsynaptic Sites of Action of mGluR8a in the mammalian retina. Invest. Ophthalmol. Vis. Sci. *43*, 1933–1940.

Krirschuk, S., and Kilb, W. (2012). GAT (GABA Transporters). In Encyclopedia of Signaling Molecules, (Springer, New York, NY), pp. 756–760.

Kruse, A.C., Ring, A.M., Manglik, A., Hu, J., Hu, K., Eitel, K., Hübner, H., Pardon, E., Valant, C., Sexton, P.M., et al. (2013). Activation and allosteric modulation of a muscarinic acetylcholine receptor. Nature *504*, 101–106.

Kufareva, I., Katritch, V., Stevens, R.C., and Abagyan, R. (2014). Advances in GPCR Modeling Evaluated by the GPCR Dock 2013 Assessment: Meeting New Challenges. Structure *22*, 1120–1139.

Labute, P. (2018). Methods of Exploring Protein–Ligand Interactions to Guide Medicinal Chemistry Efforts. In Computational Methods for GPCR Drug Discovery, (Humana Press, New York, NY), pp. 159–177.

Lecat-Guillet, N., Monnier, C., Rovira, X., Kniazeff, J., Lamarque, L., Zwier, J.M., Trinquet, E., Pin, J.-P., and Rondard, P. (2017). FRET-Based Sensors Unravel Activation and Allosteric Modulation of the GABAB Receptor. Cell Chem. Biol. *24*, 360–370.

Lehmann, K., Steinecke, A., and Bolz, J. (2012). GABA through the ages: regulation of cortical function and plasticity by inhibitory interneurons. Neural Plast. *2012*, 892784.

Lexa, K.W., and Carlson, H.A. (2012). Protein Flexibility in Docking and Surface Mapping. Q. Rev. Biophys. *45*, 301–343.

Li, J., Abel, R., Zhu, K., Cao, Y., Zhao, S., and Friesner, R.A. (2011). The VSGB 2.0 Model: A Next Generation Energy Model for High Resolution Protein Structure Modeling. Proteins *79*, 2794–2812.

Lindahl, E. (2015). Molecular Dynamics Simulations. In Molecular Modeling of Proteins, (Humana Press, New York, NY), pp. 3–26.

Lindberg, J.S., Culleton, B., Wong, G., Borah, M.F., Clark, R.V., Shapiro, W.B., Roger, S.D., Husserl, F.E., Klassen, P.S., Guo, M.D., et al. (2005). Cinacalcet HCl, an oral calcimimetic agent for the treatment of secondary hyperparathyroidism in hemodialysis and peritoneal dialysis: a randomized, double-blind, multicenter study. J. Am. Soc. Nephrol. JASN *16*, 800–807.

Lipinski, C.A., Lombardo, F., Dominy, B.W., and Feeney, P.J. (2001). Experimental and computational approaches to estimate solubility and permeability in drug discovery and development settings1PII of original article: S0169-409X(96)00423-1. The article was originally published in Advanced Drug Delivery Reviews 23 (1997) 3–25.1. Adv. Drug Deliv. Rev. *46*, 3–26.

Liu, W., Chun, E., Thompson, A.A., Chubukov, P., Xu, F., Katritch, V., Han, G.W., Roth, C.B., Heitman, L.H., IJzerman, A.P., et al. (2012). Structural Basis for Allosteric Regulation of GPCRs by Sodium Ions. Science *337*, 232–236.

Lomize, M.A., Lomize, A.L., Pogozheva, I.D., and Mosberg, H.I. (2006). OPM: orientations of proteins in membranes database. Bioinforma. Oxf. Engl. *22*, 623–625.

Loukatou, S., Papageorgiou, L., Fakourelis, P., Filntisi, A., Polychronidou, E., Bassis, I., Megalooikonomou, V., Makałowski, W., Vlachakis, D., and Kossida, S. (2014). Molecular dynamics simulations through GPU video games technologies. J. Mol. Biochem. *3*, 64–71.

Margeta-Mitrovic, M., Jan, Y.N., and Jan, L.Y. (2000). A trafficking checkpoint controls GABA(B) receptor heterodimerization. Neuron *27*, 97–106.

Marino, K.A., and Filizola, M. (2018). Investigating Small-Molecule Ligand Binding to G Protein-Coupled Receptors with Biased or Unbiased Molecular Dynamics Simulations. In Computational Methods for GPCR Drug Discovery, (Humana Press, New York, NY), pp. 351–364.

Masilamoni, G.J., and Smith, Y. (2018). Metabotropic glutamate receptors: targets for neuroprotective therapies in Parkinson disease. Curr. Opin. Pharmacol. *38*, 72–80.

McRobb, F.M., Capuano, B., Crosby, I.T., Chalmers, D.K., and Yuriev, E. (2010). Homology Modeling and Docking Evaluation of Aminergic G Protein-Coupled Receptors. J. Chem. Inf. Model. *50*, 626–637.

Meier, S.D., Kafitz, K.W., and Rose, C.R. (2008). Developmental profile and mechanisms of GABA-induced calcium signaling in hippocampal astrocytes. Glia *56*, 1127–1137.

Miao, Y., and McCammon, J.A. (2016). G-protein coupled receptors: advances in simulation and drug discovery. Curr. Opin. Struct. Biol. *41*, 83–89.

Michalon, A., Sidorov, M., Ballard, T.M., Ozmen, L., Spooren, W., Wettstein, J.G., Jaeschke, G., Bear, M.F., and Lindemann, L. (2012). Chronic Pharmacological mGlu5 Inhibition Corrects Fragile X in Adult Mice. Neuron *74*, 49–56.

Moghaddam, B. (2004). Targeting metabotropic glutamate receptors for treatment of the cognitive symptoms of schizophrenia. Psychopharmacology (Berl.) *174*, 39–44.

Mordalski, S., Kosciolek, T., Kristiansen, K., Sylte, I., and Bojarski, A.J. (2011). Protein binding site analysis by means of structural interaction fingerprint patterns. Bioorg. Med. Chem. Lett. *21*, 6816–6819.

Morley, K.C., Baillie, A., Leung, S., Addolorato, G., Leggio, L., and Haber, P.S. (2014). Baclofen for the Treatment of Alcohol Dependence and Possible Role of Comorbid Anxiety. Alcohol Alcohol *49*, 654–660.

Moustaine, D.E., Granier, S., Doumazane, E., Scholler, P., Rahmeh, R., Bron, P., Mouillac, B., Banères, J.-L., Rondard, P., and Pin, J.-P. (2012). Distinct roles of metabotropic glutamate receptor dimerization in agonist activation and G-protein coupling. Proc. Natl. Acad. Sci. *109*, 16342–16347.

Mullard, A. (2014). New drugs cost US$2.6 billion to develop.

Muly, E.C., Mania, I., Guo, J.-D., and Rainnie, D.G. (2007). Group II metabotropic glutamate receptors in anxiety circuitry: correspondence of physiological response and subcellular distribution. J. Comp. Neurol. *505*, 682–700.

Nasrallah, C., Rottier, K., Marcellin, R., Compan, V., Font, J., Llebaria, A., Pin, J.-P., Banères, J.-L., and Lebon, G. (2018). Direct coupling of detergent purified human mGlu 5 receptor to the heterotrimeric G proteins Gq and Gs. Sci. Rep. *8*, 4407.

New, D.C., An, H., Ip, N.Y., and Wong, Y.H. (2006). GABAB heterodimeric receptors promote Ca2+ influx via store-operated channels in rat cortical neurons and transfected Chinese hamster ovary cells. Neuroscience *137*, 1347–1358.

Ngomba, R.T., and van Luijtelaar, G. (2018). Metabotropic glutamate receptors as drug targets for the treatment of absence epilepsy. Curr. Opin. Pharmacol. *38*, 43–50.

Niswender, C.M., and Conn, P.J. (2010). Metabotropic Glutamate Receptors: Physiology, Pharmacology, and Disease. Annu. Rev. Pharmacol. Toxicol. *50*, 295–322.

Norinder, U., and Haeberlein, M. (2002). Computational approaches to the prediction of the blood–brain distribution. Adv. Drug Deliv. Rev. *54*, 291–313.

Nurisso, A., Daina, A., and Walker, R.C. (2011). A Practical Introduction to Molecular Dynamics Simulations: Applications to Homology Modeling. In Homology Modeling, (Humana Press), pp. 137–173.

Oldham, W.M., and Hamm, H.E. (2008). Heterotrimeric G protein activation by G-protein-coupled receptors. Nat. Rev. Mol. Cell Biol. *9*, 60–71.

Orry, A.J.W., and Abagyan, R. (2011). Preparation and Refinement of Model Protein–Ligand Complexes. In Homology Modeling, (Humana Press), pp. 351–373.

Overington, J.P., Al-Lazikani, B., and Hopkins, A.L. (2006). How many drug targets are there? Nat. Rev. Drug Discov. *5*, 993–996.

Pagano, A., Rovelli, G., Mosbacher, J., Lohmann, T., Duthey, B., Stauffer, D., Ristig, D., Schuler, V., Meigel, I., Lampert, C., et al. (2001). C-terminal interaction is essential for surface trafficking but not for heteromeric assembly of GABA(b) receptors. J. Neurosci. Off. J. Soc. Neurosci. *21*, 1189–1202.

Palczewski, K., Kumasaka, T., Hori, T., Behnke, C.A., Motoshima, H., Fox, B.A., Le Trong, I., Teller, D.C., Okada, T., Stenkamp, R.E., et al. (2000). Crystal structure of rhodopsin: A G protein-coupled receptor. Science *289*, 739–745.

Pándy-Szekeres, G., Munk, C., Tsonkov, T.M., Mordalski, S., Harpsøe, K., Hauser, A.S., Bojarski, A.J., and Gloriam, D.E. (2018). GPCRdb in 2018: adding GPCR structure models and ligands. Nucleic Acids Res. *46*, D440–D446.

Park, H.-W., Jung, H., Choi, K.-H., Baik, J.-H., and Rhim, H. (2010). Direct interaction and functional coupling between voltage-gated CaV1.3 Ca2+ channel and GABAB receptor subunit 2. FEBS Lett. *584*, 3317–3322.

Pastor, A., Jones, D.M.L., and Currie, J. (2012). High-Dose Baclofen for Treatment-Resistant Alcohol Dependence. J. Clin. Psychopharmacol. *32*, 266.

Penn, R.D., and Kroin, J.S. (1987). Long-term intrathecal baclofen infusion for treatment of spasticity. J. Neurosurg. *66*, 181–185.

Perez, D.M. (2003). The Evolutionarily Triumphant G-Protein-Coupled Receptor. Mol. Pharmacol. *63*, 1202–1205.

Pérez-Benito, L., Doornbos, M.L.J., Cordomí, A., Peeters, L., Lavreysen, H., Pardo, L., and Tresadern, G. (2017). Molecular Switches of Allosteric Modulation of the Metabotropic Glutamate 2 Receptor. Struct. Lond. Engl. 1993 *25*, 1153-1162.e4.

Phatak, S.S., Gatica, E.A., and Cavasotto, C.N. (2010). Ligand-Steered Modeling and Docking: A Benchmarking Study in Class A G-Protein-Coupled Receptors. J. Chem. Inf. Model. *50*, 2119–2128.

Pilc, A., Chaki, S., Nowak, G., and Witkin, J.M. (2008). Mood disorders: regulation by metabotropic glutamate receptors. Biochem. Pharmacol. *75*, 997–1006.

Pin, J.-P., and Bettler, B. (2016). Organization and functions of mGlu and GABAB receptor complexes. Nature *540*, 60–68.

Pittaluga, A. (2016). Presynaptic Release-Regulating mGlu1 Receptors in Central Nervous System. Front. Pharmacol. *7*.

Pol, A. van den, Wuarin, J.P., and Dudek, F.E. (1990). Glutamate, the dominant excitatory transmitter in neuroendocrine regulation. Science *250*, 1276–1278.

Polishchuk, P.G., Madzhidov, T.I., and Varnek, A. (2013). Estimation of the size of drug-like chemical space based on GDB-17 data. J. Comput. Aided Mol. Des. *27*, 675–679.

Purves, D., Augustine, G.J., Fitzpatrick, D., Katz, L.C., LaMantia, A.-S., McNamara, J.O., and Williams, S.M. (2001). The Biogenic Amines.

Rajagopal, S., Rajagopal, K., and Lefkowitz, R.J. (2010). Teaching old receptors new tricks: biasing seven-transmembrane receptors. Nat. Rev. Drug Discov. *9*, 373–386.

Rang, H.P., Ritter, J.M., Flower, R.J., Henderson, G., and Dale, M.M. (2011). Drug Discovery and development. In Rang & Dale's Pharmacology, 7e, (Edinburgh: Churchill Livingstone), pp. 726–730.

Rasmussen, S.G.F., DeVree, B.T., Zou, Y., Kruse, A.C., Chung, K.Y., Kobilka, T.S., Thian, F.S., Chae, P.S., Pardon, E., Calinski, D., et al. (2011). Crystal structure of the β2 adrenergic receptor-Gs protein complex. Nature *477*, 549–555.

Ray, K., Tisdale, J., Dodd, R.H., Dauban, P., Ruat, M., and Northup, J.K. (2005). Calindol, a positive allosteric modulator of the human Ca(2+) receptor, activates an extracellular ligand-binding domain-deleted rhodopsin-like seven-transmembrane structure in the absence of Ca(2+). J. Biol. Chem. *280*, 37013–37020.

Ripphausen, P., Nisius, B., Peltason, L., and Bajorath, J. (2010). Quo vadis, virtual screening? A comprehensive survey of prospective applications. J. Med. Chem. *53*, 8461–8467.

Robbins, M.J., Calver, A.R., Filippov, A.K., Hirst, W.D., Russell, R.B., Wood, M.D., Nasir, S., Couve, A., Brown, D.A., Moss, S.J., et al. (2001). GABAB2 Is Essential for G-Protein Coupling of the GABAB Receptor Heterodimer. J. Neurosci. *21*, 8043–8052.

Rodríguez, D., Ranganathan, A., and Carlsson, J. (2014). Strategies for Improved Modeling of GPCR-Drug Complexes: Blind Predictions of Serotonin Receptors Bound to Ergotamine. J. Chem. Inf. Model. *54*, 2004–2021.

Rondard, P., and Pin, J.-P. (2015). Dynamics and modulation of metabotropic glutamate receptors. Curr. Opin. Pharmacol. *20*, 95–101.

Rondard, P., Liu, J., Huang, S., Malhaire, F., Vol, C., Pinault, A., Labesse, G., and Pin, J.-P. (2006). Coupling of Agonist Binding to Effector Domain Activation in Metabotropic Glutamate-like Receptors. J. Biol. Chem. *281*, 24653–24661.

Rondard, P., Rovira, X., Goudet, C., and Pin, J.-P. (2017). Structure, Dynamics, and Modulation of Metabotropic Glutamate Receptors. In MGLU Receptors, R.T. Ngomba, G. Di Giovanni, G. Battaglia, and F. Nicoletti, eds. (Cham: Springer International Publishing), pp. 129–147.

Rovira, X., Malhaire, F., Scholler, P., Rodrigo, J., Gonzalez-Bulnes, P., Llebaria, A., Pin, J.-P., Giraldo, J., and Goudet, C. (2015). Overlapping binding sites drive allosteric agonism and positive cooperativity in type 4 metabotropic glutamate receptors. FASEB J. *29*, 116–130.

Ruddigkeit, L., van Deursen, R., Blum, L.C., and Reymond, J.-L. (2012). Enumeration of 166 billion organic small molecules in the chemical universe database GDB-17. J. Chem. Inf. Model. *52*, 2864–2875.

Schrödinger Release 2014-1: Canvas, version 1.9, Schrödinger, LLC, New York, NY, 2014.

Schrödinger Release 2014-1: QikProp, Schrödinger, LLC, New York, NY, 2014.

Schrödinger Release 2014-1: Phase, Schrödinger, LLC, New York, NY, 2014.

Schrödinger Release 2016-1: ConfGen, Schrödinger, LLC, New York, NY, 2016.

Schrödinger Release 2016-1: Glide, Schrödinger, LLC, New York, NY, 2016.

Schrödinger Release 2016-1: Prime, Schrödinger, LLC, New York, NY, 2016.

Schrödinger Release 2016-1: Canvas, Schrödinger, LLC, New York, NY, 2016.

Schrödinger Release 2016-3: Desmond Molecular Dynamics System, D. E. Shaw Research, New York, NY, 2016. Maestro-Desmond Interoperability Tools, Schrödinger, New York, NY, 2016.

Schrödinger Release 2016-4: Prime, Schrödinger, LLC, New York, NY, 2016.

Schrödinger Release 2016-4: LigPrep, Schrödinger, LLC, New York, NY, 2016.

Schrödinger Release 2016-4: Glide, Schrödinger, LLC, New York, NY, 2016.

Scimemi, A. (2014). Structure, function, and plasticity of GABA transporters. Front. Cell. Neurosci. *8*.

Sebastianutto, I., and Cenci, M.A. (2018). mGlu receptors in the treatment of Parkinson's disease and L-DOPA-induced dyskinesia. Curr. Opin. Pharmacol. *38*, 81–89.

Shaw, D.E., Deneroff, M.M., Dror, R.O., Kuskin, J.S., Larson, R.H., Salmon, J.K., Young, C., Batson, B., Bowers, K.J., Chao, J.C., et al. (2008). Anton, a Special-purpose Machine for Molecular Dynamics Simulation. Commun ACM *51*, 91–97.

Simms, J. (2010). Homology Modelling of G Protein-Coupled Receptors. In G Protein-Coupled Receptors, D.R. Poyner, and rk Wheatley, eds. (Wiley-Blackwell), pp. 251–273.

Siu, F.Y., He, M., de Graaf, C., Han, G.W., Yang, D., Zhang, Z., Zhou, C., Xu, Q., Wacker, D., Joseph, J.S., et al. (2013). Structure of the human glucagon class B G-protein-coupled receptor. Nature *499*, 444–449.

Sliwoski, G., Kothiwale, S., Meiler, J., and Lowe, E.W. (2014). Computational Methods in Drug Discovery. Pharmacol. Rev. *66*, 334–395.

Small-Molecule Drug Discovery Suite 2014-1: Glide, version 6.2, Schrödinger, LLC, New York, NY, 2014.

Small-Molecule Drug Discovery Suite 2014-1: Schrödinger Suite 2014-1 Induced Fit Docking protocol; Glide version 6.2, Schrödinger, LLC, New York, NY, 2014; Prime version 3.5, Schrödinger, LLC, New York, NY, 2014.

Smith, J.S., Lefkowitz, R.J., and Rajagopal, S. (2018). Biased signalling: from simple switches to allosteric microprocessors. Nat. Rev. Drug Discov.

Smith, R.D., Lu, J., and Carlson, H.A. (2017). Are there physicochemical differences between allosteric and competitive ligands? PLoS Comput. Biol. *13*, e1005813.

Sturchler, E., Li, X., de Lourdes Ladino, M., Kaczanowska, K., Cameron, M., Griffin, P.R., Finn, M.G., Markou, A., and McDonald, P. (2017). GABABreceptor allosteric modulators exhibit pathway-dependent and species-selective activity. Pharmacol. Res. Perspect. *5*, e00288.

Sun, B., Chen, L., Liu, L., Xia, Z., Pin, J.-P., Nan, F., and Liu, J. (2016). A negative allosteric modulator modulates GABAB-receptor signalling through GB2 subunits. Biochem. J. *473*, 779–787.

Swanson, C.J., Bures, M., Johnson, M.P., Linden, A.-M., Monn, J.A., and Schoepp, D.D. (2005). Metabotropic glutamate receptors as novel targets for anxiety and stress disorders. Nat. Rev. Drug Discov. *4*, 131–144.

Tehan, B.G., Bortolato, A., Blaney, F.E., Weir, M.P., and Mason, J.S. (2014). Unifying Family A GPCR Theories of Activation. Pharmacol. Ther. *143*, 51–60.

Tenorio, Y., Hernandez-Santoyo, A., Altuzar, V., Vivanco-Cid, H., and Mendoza-Barrera, C. (2013). Protein-Protein and Protein-Ligand Docking. p. 187.

Tora, A.S., Rovira, X., Dione, I., Bertrand, H.-O., Brabet, I., De Koninck, Y., Doyon, N., Pin, J.-P., Acher, F., and Goudet, C. (2015). Allosteric modulation of metabotropic glutamate receptors by chloride ions. FASEB J. *29*, 4174–4188.

Tripathi, S.K., Soundarya, R.N., Singh, P., and Singh, S.K. (2015). Comparative analysis of various electrostatic potentials on docking precision against cyclin-dependent kinase 2 protein: a multiple docking approach. Chem. Biol. Drug Des. *85*, 107–118.

Truchon, J.-F., and Bayly, C.I. (2007). Evaluating virtual screening methods: good and bad metrics for the “early recognition” problem. J. Chem. Inf. Model. *47*, 488–508.

Trzaskowski, B., Latek, D., Yuan, S., Ghoshdastider, U., Debinski, A., and Filipek, S. (2012). Action of Molecular Switches in GPCRs - Theoretical and Experimental Studies. Curr. Med. Chem. *19*, 1090–1109.

Tu, H., Rondard, P., Xu, C., Bertaso, F., Cao, F., Zhang, X., Pin, J.-P., and Liu, J. (2007). Dominant role of GABAB2 and Gbetagamma for GABAB receptor-mediated-ERK1/2/CREB pathway in cerebellar neurons. Cell. Signal. *19*, 1996–2002.

Uslaner, J.M., Kuduk, S.D., Wittmann, M., Lange, H.S., Fox, S.V., Min, C., Pajkovic, N., Harris, D., Cilissen, C., Mahon, C., et al. (2018). Preclinical to Human Translational Pharmacology of the Novel M $_1$ Positive Allosteric Modulator MK-7622. J. Pharmacol. Exp. Ther. jpet.117.245894.

Velgy, N., Hedger, G., and Biggin, P.C. (2018). GPCRs: What Can We Learn from Molecular Dynamics Simulations? In Computational Methods for GPCR Drug Discovery, (Humana Press, New York, NY), pp. 133–158.

Vogt, A.D., and Di Cera, E. (2013). Conformational selection is a dominant mechanism of ligand binding. Biochemistry (Mosc.) *52*, 5723–5729.

Wang, C., Wu, H., Katritch, V., Han, G.W., Huang, X.-P., Liu, W., Siu, F.Y., Roth, B.L., Cherezov, V., and Stevens, R.C. (2013). Structure of the human smoothened receptor bound to an antitumour agent. Nature *497*, 338–343.

Willett, P. (2006). Similarity-based virtual screening using 2D fingerprints. Drug Discov. Today *11*, 1046–1053.

Wishart, D.S. (2015). Identifying Putative Drug Targets and Potential Drug Leads: Starting Points for Virtual Screening and Docking. In Molecular Modeling of Proteins, (Humana Press, New York, NY), pp. 425–444.

Wood, M.R., Hopkins, C.R., Brogan, J.T., Conn, P.J., and Lindsley, C.W. (2011). "Molecular Switches" on mGluR Allosteric Ligands That Modulate Modes of Pharmacology. Biochemistry (Mosc.) *50*, 2403–2410.

Wootten, D., Christopoulos, A., and Sexton, P.M. (2013). Emerging paradigms in GPCR allostery: implications for drug discovery. Nat. Rev. Drug Discov. *12*, 630–644.

Wu, H., Wang, C., Gregory, K.J., Han, G.W., Cho, H.P., Xia, Y., Niswender, C.M., Katritch, V., Meiler, J., Cherezov, V., et al. (2014). Structure of a Class C GPCR Metabotropic Glutamate Receptor 1 Bound to an Allosteric Modulator. Science *344*, 58–64.

Xue, C., Hsueh, Y.-P., and Heitman, J. (2008). Magnificent seven: roles of G protein-coupled receptors in extracellular sensing in fungi. FEMS Microbiol. Rev. *32*, 1010–1032.

Xue, L., Rovira, X., Scholler, P., Zhao, H., Liu, J., Pin, J.-P., and Rondard, P. (2015). Major ligand-induced rearrangement of the heptahelical domain interface in a GPCR dimer. Nat. Chem. Biol. *11*, 134–140.

Yin, S., Noetzel, M.J., Johnson, K.A., Zamorano, R., Jalan-Sakrikar, N., Gregory, K.J., Conn, P.J., and Niswender, C.M. (2014). Selective Actions of Novel Allosteric Modulators Reveal Functional Heteromers of Metabotropic Glutamate Receptors in the CNS. J. Neurosci. *34*, 79–94.

Youden, W.J. (1950). Index for rating diagnostic tests. Cancer *3*, 32–35.

Yuan, S., Filipek, S., Palczewski, K., and Vogel, H. (2014). Activation of G-protein-coupled receptors correlates with the formation of a continuous internal water pathway. Nat. Commun. *5*, 4733.

Höltje, H.-D. (2008). Molecular modeling: basic principles and applications (Weinheim: Wiley-VCH).

Paper 1

Paper 2

Paper 3